DMTA investigation of solvents effects on viscoelastic properties of porous $CaCO_3$- SBR latex composites

F. Touaiti[a], P. Alam[a], M. Toivakka[a] and M. P. Ansell[b].

[a] Laboratory of Paper Coating and Converting, and Center for Functional Materials, Åbo Akademi University, Porthansgatan 3, Turku 20500, Finland

[b] Department of Mechanical Engineering, University of Bath, Bath BA2 7AY, United Kingdom

Abstract

The impact of water, linseed oil and mineral oil solvents on the viscoelastic properties of calcium carbonate - caboxylated styrene buradiene ($CaCO_3$-SBR) porous coatings has been investigated using a dynamic mechanical thermal analysis (DMTA) technique in single cantilever mode from -30°C to 70°C. Water and oils reduce the glass transition temperature (Tan Delta peak) of pure latex. Oils increase the rubbery storage modulus which may be due to oxidation leading to entangled chains that contribute to resistance to deformation. Scanning electron microscopy (SEM) was used to visualise the porous structure of these composites. Further analysis using Image J software showed that increasing the latex content results in the development of small circular (2D) pores. The effect of solvents on the elastic response of coating depends on the chemical nature of the solvent and its molecular size. Linseed oil and water decreased the composite's storage modulus for 5 pph, 10 pph and 15 pph coatings, in contrast to mineral oil which had a negative impact at relatively higher latex content (50 pph). The drop in the strength and storage modulus of solvent saturated latex coatings is proportional to the solvent surface tension to viscosity ratio. The low values of storage modulus were interpreted as low adhesion between $CaCO_3$ particles and the styrene-butadiene matrix. For low latex content coatings, low storage modulus is due to porosity which forms suitable sites for cracks initiation and propagation through the coatings. At higher latex volume fraction coatings the composite behaviour approaches that of pure latex.

Keywords: Porous composites; DMTA; viscoelasticity; pigment coating; linseed oil; mineral oil; water;

Background

Paper coating is an important stage before printing as both the quality and the runability of printing depend on the coating layer structure and properties. The coating layer consists of inorganic pigments (Calcium carbonates, clay ...) bonded together by polymer latex network (styrene copolymers) and porosity that arises from the pigments packing (occupy around 20% of the total composite volume). Porosity has a great impact on many paper properties including light scattering, mechanical strength and ink setting during printing. The mechanical properties of paper are mostly dependant on the coating layer as it ensures enough strength for paper to be processed. For example during printing, the paper passes through various nips

where it is subjected to compressive and tensile stresses (nip entrance and exit) under the impact of water and other ink oils.

Previous research concerning the effect of printing inks (containing a mobile solvent phase) on pigment coatings has shown that the two main factors affecting ink setting via diffusion and capillary flow are latex chemistry and pore structure [1]. Latex chemistry determines the strength of interactions between the ink mobile phase, i.e. solvent and the bulk polymer. Fast ink setting in high latex volume fraction coatings is related to the swelling of latex. Solvents diffuse easily due to strong interactions between the polymer and the solvent molecules [2]. Van Glider et al report that the interactions between latex and solvent molecules have a significant impact on the coating pick strength (the maximum force the coating surface can withstand before it separates from the base paper). Latex with a high surface energy (high polarity) will show a more marked difference between the solubility parameter of the latex and the solvent and thus will have greater resistance to solvent attack [3].

Pore structure (pore size, porosity level) influences ink setting at lower latex volume fractions. Experimental studies have shown that ink setting is faster in smaller pores (high capillary pressure) as compared to larger ones [4, 5]. Viscosity plays a great role in the absorption of oil into coatings. Khinnavar and Harrogoppad [6-7] showed that diffusion through polymer matrices is solvent size dependent. Solvent size and viscosity are interrelated.
Studying the interaction between the mobile solvent phase and the coating structure is of great importance to both the printing quality and the mechanical strength of papers. Solvent diffusion decreases adhesion between the latex and pigment particles. The aim of this communication is to elucidate the effects of linseed and mineral oils, as well as water, on the viscoelastic and adhesive properties of coatings consisting of low (5 pph, 10 pph and 15 pph) and high (50pph) latex weight fractions. As these liquids are intensively used in the printing process as fountain solution (water) and ink mobile phase (linseed and mineral oils). Dynamic mechanical thermal analysis (DMTA) techniques are used to fulfil this objective.

Materials and methods

The styrene butadiene latex used in this research is manufactured by Dow Deutschland Anlagengesellschaft GmbH. This latex has a glass transition temperature of 8°C measured by Differential Scanning Calorimetry and a particle size of 132 nm. During emulsion polymerisation acrylic acid was added to the composition (5 weight % of total monomer weight) to control the chemical functionality and particle – particle polymer interdiffusion while drying. [8]. It was also shown that the latex spreading above Tg depends on the degree of carboxylation [9].

The coating formulations consists of ground calcium carbonate (GCC) *Carbital™ 90* pigments produced by Imerys Minerals Ltd and carboxylated styrene butadiene latex manufactured by Dow chemicals. Both constituents were mixed in controlled ratios to prepare 5pph, 10pph, 15pph and 50 pph latex slurries. The coating mixtures were injected into a pressure filtration rig to produce thick coating tablets that were cut afterwards into appropriate size for DMTA test. Further details of sample manufacturing can be found in a previous communication [10].

The oils used are commercial linseed and mineral oils delivered by Imerys Minerals Ltd. Table 1 summarises some of their physical properties. γ_s and γ_{SBR} are the surface tensions of solvent and the carboxylated styrene butadiene latex respectively, and η is the solvent

viscosity. The surface tension of latex film has been measured using the Sessile Drop method performed by a CAM 200 optical contact angle meter [11]. The measurement was performed after 1s from water droplet application on the latex film surface. The measured value agrees with that indicated by the latex producer (49 mN/m). The oil viscosities were taken from their data sheets.

Table 1. Some physical properties of latex and different solvents used in this study

In Table 1, the numerator (γ_s- γ_{SBR}) is related to the solubility of latex in the solvent as reported in literature [3]. Furthermore Bonn et al, found a strong correlation between the values of cohesive energy density and surface tension in polymers [12], these facts justify the use of surface tension as an indication of solubility of latex in different liquids. The denominator (η) is related to the solvent molecular size, beyond the chemistry consideration the bigger the molecular size the higher the resistance to flow (viscosity).

To study the solvents absorption in latex and these coatings, three 100 ml beakers were filled with de-ionized water, linseed oil and mineral oil. Pure latex and coating samples were immersed in these beakers after recording their initial weights. The solvent uptake rate is measured in terms of weight gain within 24, 48 and 72 and 96 hours.

DMTA is generally used to measure viscoelastic properties like the storage modulus (material elastic response), the loss modulus (viscous response) and loss factor (damping) with respect to temperature and/or frequency. These tests were conducted in single cantilever bending mode at a frequency of 1 Hz, a heating rate of 3°C/min and amplitude of 0.1% strain. Coating samples were immersed in different solvents (mentioned in table 1) for 24 hr before testing. The reported glass transition temperature was calculated from the loss modulus peak as suggested in literature [13].

Coating microstructure

Figure 1, shows a close view of 5 pph latex coatings (8 % latex volume fraction) bulk region in back scattering scanning mode (BSEM). The pore network has a pore size varying from 0.5 to 2 µm. In the 10 pph latex coating sample (15 % latex volume fraction), the structure of the bulk porous network is less open thus indicating a lower porosity as compared to the 5 pph coating. Moreover, the pore size is smaller, ranging from 0.25 to 1 µm (Figure 2). The calcium carbonate pigments are indicated by blue arrows in Figure 5.

As expected, these SEM images show that increasing the latex volume fraction reduces both the porosity and the average pore size.

Figure 1: Example of BSEM image showing the microstructure of cross-section of 5 pph latex bulk coating, the pores, the calcium carbonate pigments and the latex are shown with red, blue and green arrows respectively.

Figure 2: Example BSEM image showing the microstructure of cross section of 10 pph latex bulk coatings.

Image J software was used for a statistical analysis of the coating microstructure analysis. The 5 pph latex coating and 10 pph latex coating microstructures were analysed using 5 BSEM images in each case. The results are averaged from the sample set and presented in Table 2. Example images are shown in Figure 3.

Table 2. Image J analysis of 5 pph latex and 10 pph BSEM images

Figure 3. The pores distribution from Image J analysis software, upper image shows the 5 pph latex coatings where the lower shows the 10 pph coatings (magnification X10 000).

Both the pore area fraction and the average pore size, Table2, show that 5 pph coatings have a more open pore structure than 10 pph coatings. The circularity and the Feret diameter indicate the effect of latex inclusion on the pore geometry. As the latex content is increased, pores became more circular (2D). This in turn shows that latex tends to close off pores in higher latex content coatings.

Coatings- solvent absorption

The coatings-solvent absorption curves are shown in Figure 4. At lower latex content water and linseed oil are quickly absorbed into the samples until saturation is reached at around 24 hr. As the latex content increases, samples tend to absorb mineral oil faster than other solvents. At the 10 pph latex level water, mineral oil and linseed oil have almost similar absorption rate.
Latex samples showed a higher water absorption rate compared to oils and saturation was not reached within the time of this experiment. The linseed oil absorption rate drops with time this may be due to physical bonding rising from chain entanglement between latex chains and the oil molecules or chemical bonding reaction between the hydroxyl groups of linseed oil and carboxylic latex groups as described by Hess et al [14].

Figure.4: Solvents absorption curves for composite (top) and pure latex (bottom) samples.

Dynamic mechanical thermal analysis

Damping properties of pure latex

The decrease in the glass transition temperature of pure latex samples immersed in water, mineral oil and linseed oil is an indication of a plasticising effect (Figure 5). As the solvents

diffuse into the latex they increase the polymer intermolecular free volume. As a consequence the glass transition temperature drop as the polymer chains gain free space and are more mobile [15]. The width of Tan Delta (loss factor) peak is an indication of the molecular structure of the polymer. A wide peak like that of mineral oil soaked latex indicates high disorder in the latex structure (more chains are entangled). When the chains gain sufficient energy (as temperature increases) to overcome both the intermolecular forces and the chain entanglements, higher molecular mobility is observed (above 50°C).

Figure.5: Loss factor curves for pure SBR latex immersed in different solvents.

Many researchers have assumed that diffusion of solvent into latex can be described by Fick´s third law. Diffusion coefficients used in this law describe the rate of solvent diffusion into the polymer film. Fouchet et al. reported a mineral oil diffusion coefficient of 5.53×10^{-14} m^2/s at room temperature [16]. Richard et al reported a water diffusion coefficient of $10^{-8} m^2/s$ [17].
Both the size and the chemical nature of the solvent molecules influence the value of the diffusion coefficient. Therefore as a function of its molecular weight, linseed oil diffuses more slowly than mineral oil as proven by the absorption curves in Figure 14. Water diffuses faster than both oils [17-18].

As a strong polar solvent, water actively interacts with polar carboxylic groups within the latex which are primarily located at the surface of the latex particles. Linseed oils are less polar and have lower levels of interaction as compared with water [17, 19]. Contrary mineral oil is a non-polar solvent and tends to diffuse through butadiene blocks [19, 21]. The particles - latex interactions in pigment coating are known to be of acid-base nature, which implies that polar liquids do have an effect on the interfacial strength in these composites.

In Figure 6, the glassy state storage modulus seems more or less constant for all the samples Due to low testing amplitude (1Hz) and the low polymer chains mobility (no enough energy), no significant solvent impact was observed. In the rubbery state, mineral oil raises the modulus to twice that of dry samples (at 50°C). Mineral oil diffuses into butadiene blocks and subsequent oxidation stimulates the formation of intrinsic peroxide bonds and intermolecular entanglements with the latex, which stiffen the material [22, 23].

This is not observed in the case of the other solvents, perhaps because they are attracted more towards carboxylated domains, which occupy a lower volume fraction of the polymer than butadiene. The level of disorder is lower than that of latex immersed in mineral oil.

Figure.6: Storage modulus curves for pure SBR latex immersed in different solvents.

Dynamic thermal analysis of composite samples

While preparing the coating formulation, the pigments are mixed together with latex particles. During drying process, latex particles fuses together to form a rubber film that binds the inorganic pigments together. Latex volume fraction plays a decisive role in the mechanical properties of such composite as Figure 7 illustrates. Increasing the latex volume fraction induces higher storage modulus mainly by reducing the porosity (latex tends to fill the pores).

Figure 7 indicates the existence of an optimum (effective) latex volume fraction beyond which no increase in the storage modulus will be observed. This result emphasises the effect latex has on the pigment- pigment bonding as well as the continuity of the latex network on the mechanical properties of these composites as mentioned by Alam [24].

In 15 pph latex coatings latex network was more spread and continues compared to 5 pph and 10 pph latex coatings, and have high pigment volume fraction (50 % $CaCO_3$) compared to 50 pph latex coatings (40% $CaCO_3$). These characteristics induced the higher storage modulus in the whole temperature range. Whereas in 50 pph latex coatings more viscous flow was observed at the rubbery region due to the fact that the latex volume fraction was higher than the effective concentration which led to separate latex regions within the structure that flows under heat rather than contribute to the composite (coating) elastic response .

Figure 7: Effect of latex volume fraction on storage modulus of dry coatings.

The effect of water, mineral oil and linseed oil on the storage modulus of 5 pph latex coatings is shown in Figure 8**.**

Figure. 8. Storage modulus of 5 pph latex coatings as dry and as immersed in different solvents.

In the glassy state below 0°C, water saturated coatings have the highest storage modulus. This is due to ice formation at these temperatures. Ice increases the storage modulus because it occupies the pore space and contributes to load resistance. In single cantilever bending, one side of the sample is in compression. Since the young modulus of ice at 1Hz is approximately 8GPa [25], the effective composite modulus is raised as a function of the reinforcing effects of ice. As the temperature increases, ice melts and the storage modulus drops below that of the dry coating.

Mineral oil plasticises latex chains (Figure 5), thus there is a decrease in the storage modulus as the temperature increases. Linseed oil has a disastrous effect on the coating storage modulus as it attacks the pigment-latex interfaces, and creates discontinuity in the composite matrix.

It should be noted that water does not have the same effect as linseed oil even though both are polar solvents. Water in its crystalline state (ice) forms a separate phase within the coating. As ice melts the water molecules tend to diffuse into the interfacial areas at c.a. 5°C, which is illustrated by the storage modulus drop that decreases then stabilises at c.a. 30°C. It is possible that

a) The rate of diffusion to interfaces is not high enough for the effect to be noticed as in the case of linseed oil.
b) Water is lost through evaporation, unlike linseed oil.

Figure 9. Effect of water, mineral and linseed oils on the damping properties of 5 pph latex coatings.

On observing Figure 9, it can be concluded that both linseed oil and mineral oil create higher molecular disorder and heterogeneity in the latex. This is evidenced by the broad loss factor peaks. This is due to their molecular sizes as compared with water (which shows lower heterogeneity). Water has a small peak around 0ºC which is due to ice melting. Pinhas et al [26] have found similar peaks arising as ice melts in gelatin. They suggested that water released from ice does not (within the DMTA experiment time scale) diffuse and fully equilibrate through the sample. This can further explain why water does not show a higher damping peak which is associated with significant displacement at significant application of force.

Mineral oil and linseed oil immersed coatings have higher loss factor peaks as compared to the dry coatings and the water immersed coatings. This is due to coating structure modification as both oils respectively soften the butadiene domains in the SBR latex molecules and weaken the latex- particle interfaces.

The effects of different solvents on the storage modulus of 10 pph are shown in Figure 10.

Figure 10. Effect of different liquids on 10 pph latex coatings storage modulus.

The dry coating in Figure 10 has the highest storage modulus at all temperatures as compared to any of the solvent immersed coatings. The 24 hour saturation time allows water to attack interfaces and cause de-bonding. The pore network is less open in 10 pph coatings than in 5 pph coatings, Table 2. More pores are closed in 10 pph coatings and therefore water does not occupy pore spaces as easily as it did in 5 pph coatings. Hence the effects of load resistance from large volumes of ice are not present as in 5 pph coatings. The linseed oil immersed coating, again showed the lowest storage moduli to c.a. 25°C from which point the water saturated coating storage modulus was marginally lower.

Linseed oil weakens the particle-polymer interfaces. In 5 pph coatings, the open pore network allows more oil to reach these interfaces than is possible with 10 pph coatings. As a result the storage modulus is not reduced as significantly in 10 pph coatings as it is in 5 pph coatings.

Figure. 11. Effect of different solvents on the damping of 10 pph latex coatings.

Dry coatings are stiffer than solvent immersed coatings. Water immersed coating has no ice melting peak (Figure 11). This is due to the less open pore structure as at 10 pph the pores are smaller and the porosity is lower than 5 pph coatings.

The glass transition temperature of mineral oil immersed coating exemplifies the plasticising capability of this solvent (13 degrees lower than dry sample). This coating experiences a clear increase in damping (loss factor) at higher temperatures. Essentially, greater disorder is introduced to the butadiene domains in the presence of mineral oil chains.

Linseed oil saturated coatings have higher damping at low temperatures (more internal friction) than the other samples. This is due to weakening at particle-latex interfaces. As temperature increases, latex chains at interfaces raise the internal friction (broad loss factor peak).

The effect of water, mineral oil and linseed oil on the storage modulus of 15 pph latex coatings is shown in Figure 12.

Figure 12. Effect of different solvents on storage modulus of 15 pph latex coatings

For 15 pph coatings, Figure 13, the impact of different liquids on the storage modulus is similar to the 10 pph storage modulus-temperature curves (see Figure 10). As the latex fraction increases, the pores become smaller and the interfacial areas decrease as more latex covers the calcium carbonate pigments. Polar solvents tend to attack the interfaces. This weakens the composite and decreases the storage modulus. Mineral oil diffuses into the latex butadiene domains (it softens them as shown in Figure 5) and softens the coatings.

Figure 13. Effect of different solvents on the damping of 15 pph latex coatings.

In 15 pph coatings, all solvents have similar effects on the coating glass transition temperature. The oils show a broader peak due to the molecular structure (long chains) compared to water (small molecule). The effect of the chain length on the damping properties can be clearly seen. Small water molecules with high polarity attack the coating interfaces and induce greater softening. Mineral oil has smaller chains compared to linseed oil and diffuses into the butadiene domains thus softening the latex within the coating. Linseed oil has a high viscosity and weakens the interfaces thereby softening the coatings to a lower extent than the other solvents.

The effect of different solvents on the 50 pph coating storage modulus is shown in Figure 14.

Figure 14. The effect of water, linseed oil and mineral oil on the storage modulus for 50 pph latex coatings.

At 50 pph latex weight fraction, water (small molecule) has a greater impact on the storage modulus than the oils. The molecular size is of considerable importance in view of interfacial weakening. It is suggested that water attacks more interfacial sites compared to linseed oil. Oil, comprising long molecules, may develop entangled networks with latex chains. These entangled chains resist deformation and balance, to some extent the detrimental effects of the oils on interfaces. Hence the storage modulus is higher in the oil immersed coatings than with water immersed coatings.

Figure 15: The effect of solvents on the damping properties of 50 pph latex coatings.

The linseed oil immersed coating shows rigid behaviour (low loss factor) when compared to dry and other solvent immersed coatings. This could be due to the oxidation of linseed oil which helps the formation of entangled network [22, 23]. It is unlikely that strong interactions develop between the carboxylic parts of the latex and the linseed oil molecules. Such interactions will weaken as temperature increases, which is not the case here.

Water immersed coating exhibit higher damping (Figure 15) since water attacks the pigment-latex interfaces [27] and increases internal friction.

Discussion

The viscoelastic properties of pigment coatings are strongly dependent on three main factors namely; the solvent characteristics (polar or non-polar, short or long molecule), the latex volume fraction and the coating microstructure.

At lower latex volume fractions, coatings have a very open pore network and the permeability of different solvents is higher than in high latex volume fraction coating. This in turn favours higher volume rates of solvent diffusion into latex and at particle-latex interfaces. Even though, the mineral oil absorption rate depends greatly on the latex volume fraction within the composites, the porous structure of the coating increases the volume rate of diffusion of mineral oil as more latex surface is exposed within the structure. This softens the latex butadiene domains which reduced the storage modulus. At lower latex volume fractions the results agreed with the conclusions of Husband [27] and Van Glider [3] who highlight the adverse effect of polar solvent on kaolin-$CaCO_3$-SB latex coating strength, measured using an ink-splitting force test.

As the latex volume fraction increases, the negative effect of mineral oil on the strength becomes apparent. On the other hand, this negative effect decreases as interfacial areas exposed to its attack are decreased. Linseed oil also has a higher viscosity than the other solvents and is less permeable in the 'less open' pore networks. Water contrarily, can permeate and diffuse with relative ease.

Due to its strong polarity water has a catastrophic effect on the stiffness of these coatings. Oils do not have as detrimental effect as water does on storage modulus at higher latex volume fraction coatings. It is possible that above the glass transition temperature, oils give rise to an entangled network. The impact of solvent at higher latex volume fractions seems to agree with the studies of Khinnavar [6] and Harrogoppad [7], who concluded that alkane based solvents with short molecules diffuse faster in SBR membranes.

Most printing processes are conducted at room temperature. This lies within the glass transition region of the coatings studied here (3 °C to 30°C). The storage modulus drop within this region can be a means by which the levels of weakening solvents have on coating strength can be characterised qualitatively. Sharp drop in the storage modulus reflect interfacial weakening due to solvent impact. As latex chains gain greater mobility [13] in this region, only chains bounded to the CaCO3 particles resist the deformation and contribute to the elastic response; more bounded chains leads to low decay in the storage modulus. As these bonds deteriorate, chains gain greater freedom of mobility. This favours increased viscous behaviour within the material and consequently reduces the stiffness. Using the storage modulus drop ($\Delta E_S' = E'_{20°C} - E'_{30°C}$) in the glass transition region, the impact of solvent on coating strength at a printing process temperature can be evaluated. $E'_{20°C}$ and $E'_{30°C}$ are the storage moduli at 20°C and 30°C respectively. Higher values of $(\Delta E_S')/ (\Delta T)$ indicate higher effects of solvent attack as the strength drops faster with respect to temperature.

From the above DMTA results it could be suggested that both: the chemical nature (polar, non-polar) of the solvent and its molecular sizes (small, large) are the main factors that affect the mechanical and viscoelastic properties of these coatings. Another aspect to take into consideration is that these coatings have been immersed in solvent for 24hours. Within this time the solubility of latex in the solvent will also affect the coating strength. To combine these two effects a solvent characteristic ratio $(\gamma_s - \gamma_{SBR})/ \eta$ has been used. This ratio is shown in Table 1. Similar ratios have already been used to evaluate ink absorption in pigment coatings [28]. The plot of storage modulus drop versus the solvent characteristic ratio is shown in Figure 16 for the range 20°C-30°C.

Figure.16. Effect of solvent physical properties on storage modulus drop for different coatings.

As the solvent characteristic ratio increases, a greater drop in the storage modulus can be observed. Water has the most detrimental effect on the coatings storage modulus. At lower latex volume fraction coatings, the weakening effect of water on the coatings is low because of ice formation. Increasing the latex content leads to a tighter structure where water diffuses more into the coating thus reduces in the elastic properties. Generally the drop due to mineral oil increases with latex volume fraction (it overcomes the effect of water at 50 pph). Linseed oil showed a lower effect compared to mineral oil and water. This may be due to its viscosity that prevents the diffusion of polar oil molecules into the coating structure. In summary, solvents with small polar molecules have a more devastating effect on the adhesion and elastic response than larger molecules of non-polar solvents.

Conclusions:

The investigation of solvent impact on viscoelastic properties of $CaCO_3$-SBR latex leads to the following conclusions:

1- The absorption of water and linseed oil by coating depends strongly on porosity, whereas latex volume fraction is the important factor for mineral oil absorption.
2- All solvents reduce the latex glass transition temperature (plasticising effect).
3- Water as small polar solvent is more destructive to the microstructure at higher latex volume fractions, whereas in highly porous coatings it forms ice that raises the storage modulus below 0°C.
4- Linseed oil diminishes the storage modulus of low latex content coatings, as it attacks the particle-latex interfaces and causes interfacial weakening.
5- Mineral oil has a negative effect on storage modulus at high latex volume fractions.
6- Coating strength and elasticity has a strong relationship with the surface tension and viscosity of the solvent in which the coating is immersed.

References

1. Y. Xiang, D. W. Bousfield, The influence of ink-coating interaction on final print density in multicolor offset printing, TAPPI International Printing and Graphic Arts, 2000, pp 299-309.

2. Y. Xiang, D. W. Bousfield, The influence of coating structure on ink tack development, Journal of Pulp and Paper Science, 2000, vol 26 pp 221-227.
3. R. L. Van Glider and R. D. Purfeerst, Latex binder modification to reduce coating pick on six-color offset press, TAPPI Journal, 1994, 230-239.
4. Y. Xiang, D. W. Bousfield, J. Kettle and L. Hultgren, Effect of latex swelling on ink tack build and ink gloss dynamics of coatings, TAPPI International Printing and Graphic Arts, 2000, pp 139-151.
5. P. Gane, E. Seyler, Some novel aspects of ink/paper interaction in offset printing, TAPPI Journal 1994.
6. R. S. Khinnavar and T. M. Aminabhavi, Diffusion and sorption of organic liquids through polymer membranes I, Journal of Applied Polymer Science, 1991, vol 42, 2321-2328.
7. R. S. Harrogoppad and T. M. Aminabhavi, Diffusion and sorption of organic liquids through polymer membranes II, Neoprene, SBR, EPDM, NBR, and natural rubber versus n-alkanes, Journal of Applied Polymer Science, 1991, vol 42, 2329-2336.
8. J. L. Keddie, A. F. Routh, Fundamentals of latex film formation, 1st Edition, 2010, ISBN: 978-90-481-2844-0
9. V. Garnier, A. Sartre, Ordering and adhesion of latex particles on model inorganic surfaces, Langmuir, 1995, vol 11, pp 2179-2186
10. F.Touaiti, P. Alam, M.Toivakka, D. Bousfield Polymer chain pinning at interfaces in $CaCO_3$–SBR latex composites, Materials Science and Engineering: A, April 2010, vol 527, Issue 9, 15 , Pages 2363-2369.
11. M. Mondon , C.Ziegler, Water Contact Angle during Impression Material Setting, The International Journal of Prosthodontics, Volume 16, Number 1, 2003
12. R. Bonn and J. J. Vanaartsen, Solubility of polymers in relation to surface tension and index of refraction, European Polymer Journal, 1972, Vol. 8, pp. 1055-1066.
13. J. D. Menczel, R. B. Prime, Thermal analysis of polymers: fundamental and applications, Wiley 2009, ISBN 978-0-471-76917-0.
14. P. S. Hess and G. A. O'Hare, Oxidation of linseed oil; temperature effect, Industrial and Engineering Chemistry, Vol 42, No 7, 1950, p 1424-1431
15. J. M. G. Cowie, Polymers: chemistry and physics of modern materials, 2nd edition UK, 1991.
16. B. Fouchet, Diffusion of mineral oil in styrene-butadiene polymer films, Journal of Applied Polymer Science, 2008, vol 111, pp 2886-2891.
17. J. Richard, C. Mignaud, K. Wong, Water vapour permeability, diffusion and solubility in latex films, Polymer International, 2007, vol 30 issue 4, pp 431-439.
18. P.C. Hiemenz, T. P. Lodge, Polymer chemistry 2nd edition CRC, 2007.
19. M. H. Schneider, Hygroscopicity of wood impregnated with linseed oil, Wood Science and Technology, 1980, vol 14, pp 107-114.
20. L. S. Flosenzier and J. M Torkelson, Influence of molecular weight and composition on the morphology and mechanical properties of SBS-Polystyrene-Mineral oil blend, Macromolecules, 1992, vol 25, pp 735-742.
21. Sebastiao V. Canevarolo, Luiz H. C. Mattoso. Preferential plasticization of SBS triblock copolymer, Britain Polymer Journal, 2007, vol 22, pp 137 – 141.
22. M. Lazzari, O. Chiantore, Drying and oxidative degradation of linseed oil, polymer degradation and stability ,1999, vol 65, pp 303-313
23. J. Mallegol, J. Lemaire, J. L. Gardette, Progress in Organic Coatings, 2000, vol 39, pp 107-113.
24. P. Alam, A mixtures' model for porous particle-polymer composites, Mechanical research communication, 2010, vol 37, pp 389-393.

25. L. W. Gold, Engineering properties of fresh-water ice, Journal of Glaciology, 1977, vol 19, no 81 p 197-212.
26. M. F. Pinhas, J. M. Blanshard, W. Daerbyshire and J. R. Mitchell, The effect of water on the physicochemical and mechanical properties of gelatine, Journal of Thermal Analysis, 1996, vol 47, pp 1449-1511.
27. J. C. Husband, J. S. Preston, D. Blair, new insight into the printing strength of calcium carbonate coatings, 23rd PTS coating Symposium, Baden –Baden, 2007, pp 1-14
28. L. Gate and W. Windle, Absorption of oils into porous coatings, fundamental properties of paper related to its uses. Ernest Benn Ltd, London, UK, pp 438.

Figure 1(Example of BSEM image 5pph)
Click here to download high resolution image

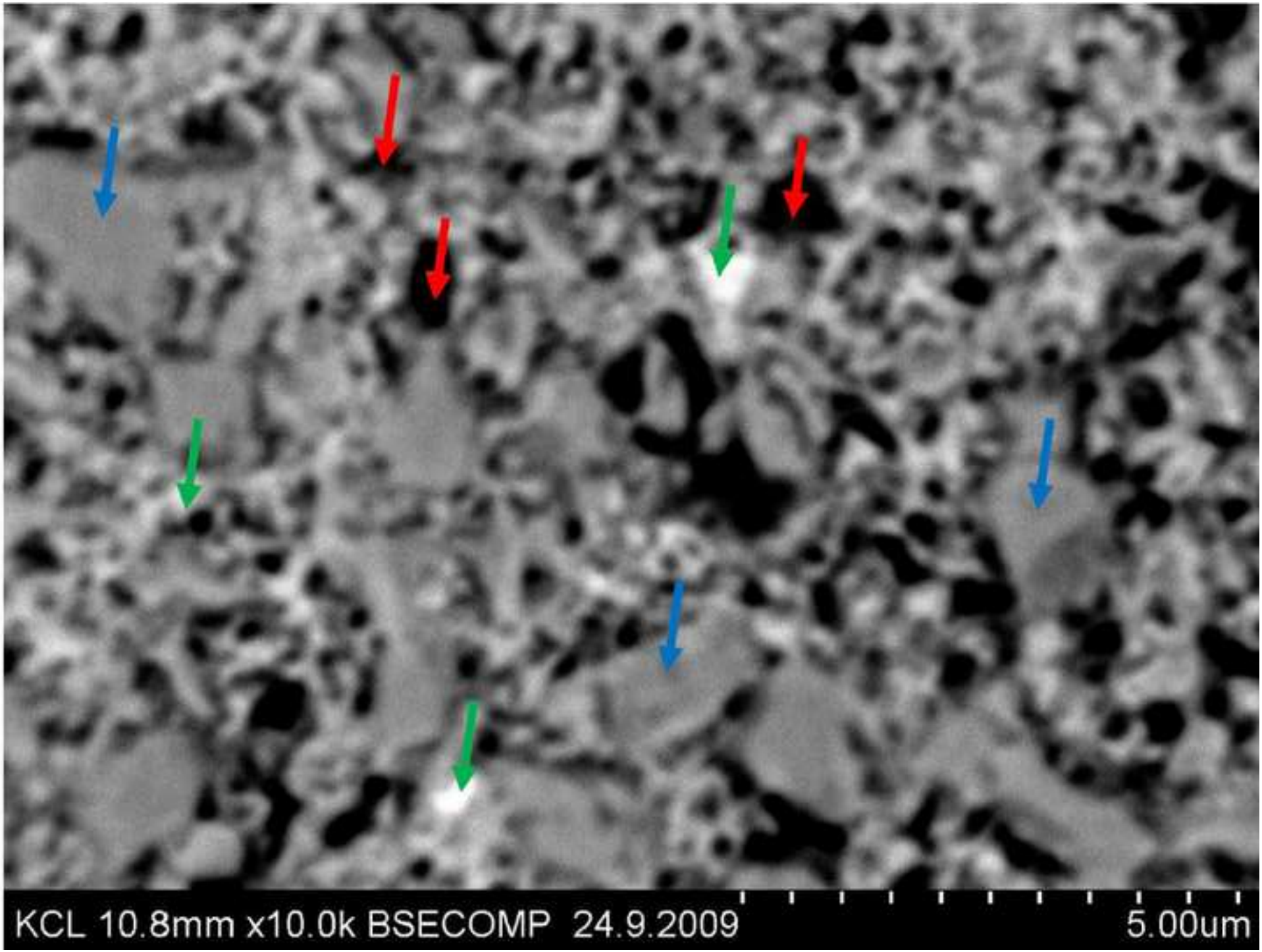

Figure 2(Example of BSEM image 10pph)
Click here to download high resolution image

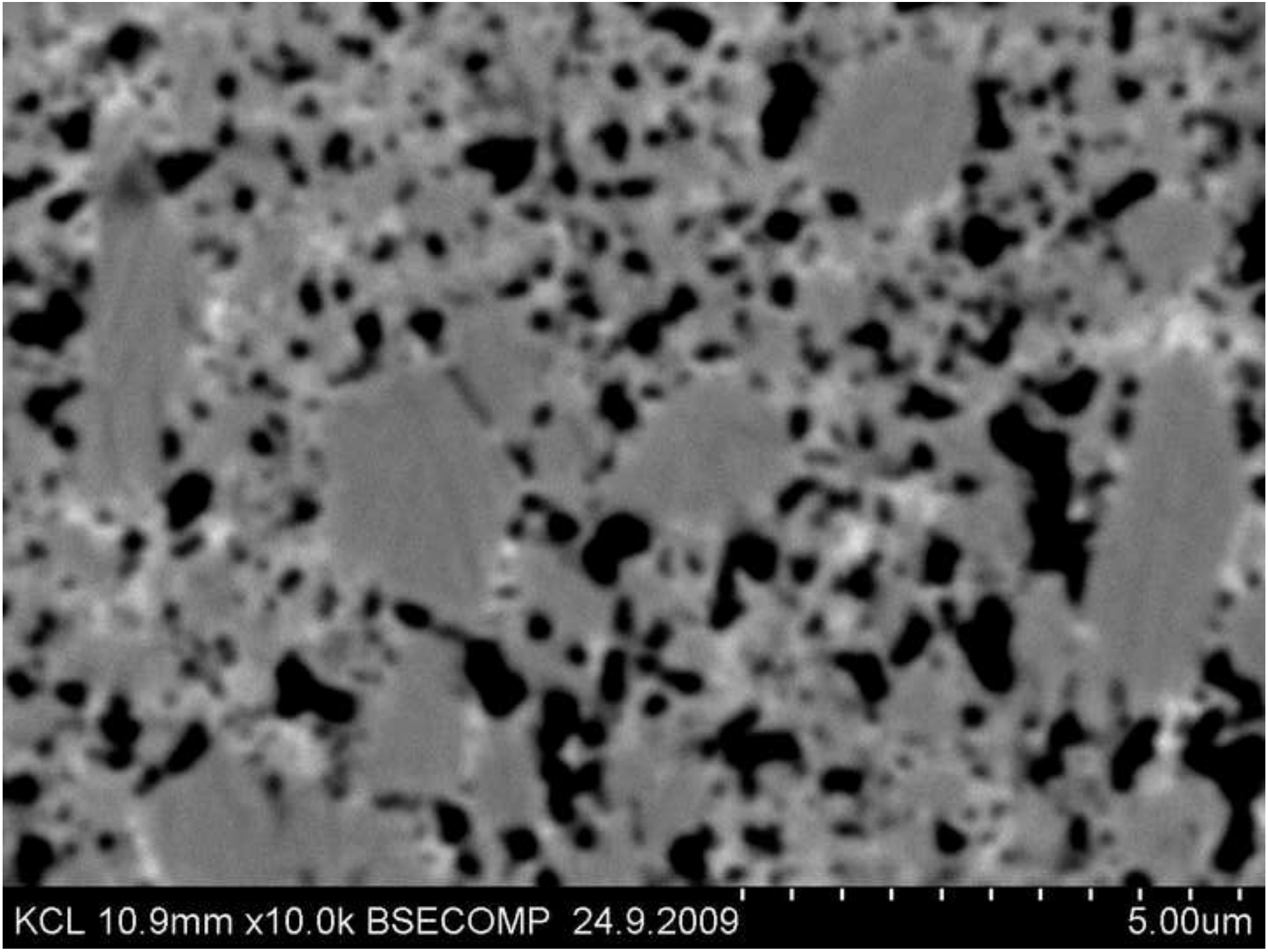

Figure 3 (image analysis of 5 pph and 10 pph)
Click here to download high resolution image

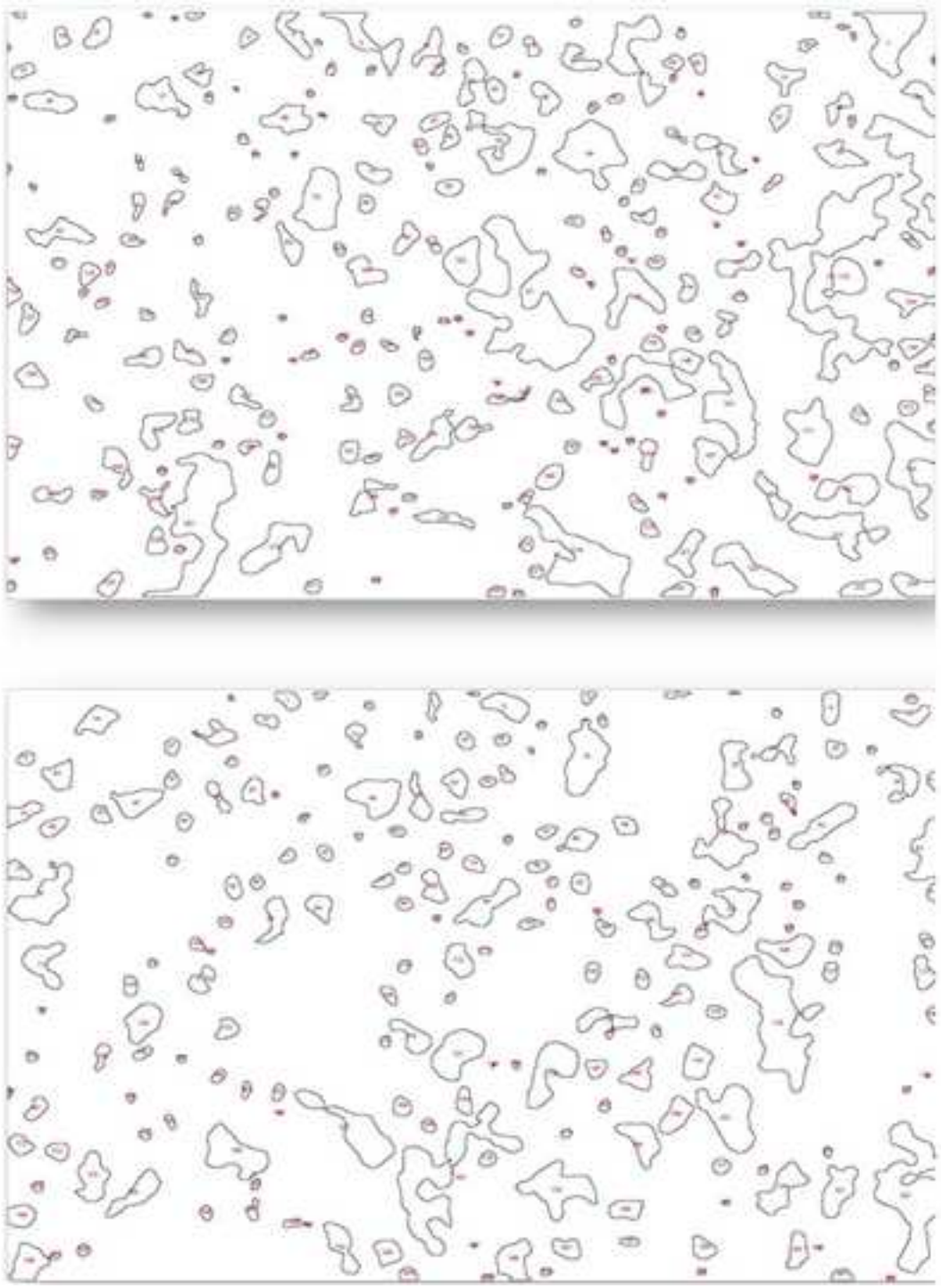

Figure 4 (solvents absorption curves)
Click here to download high resolution image

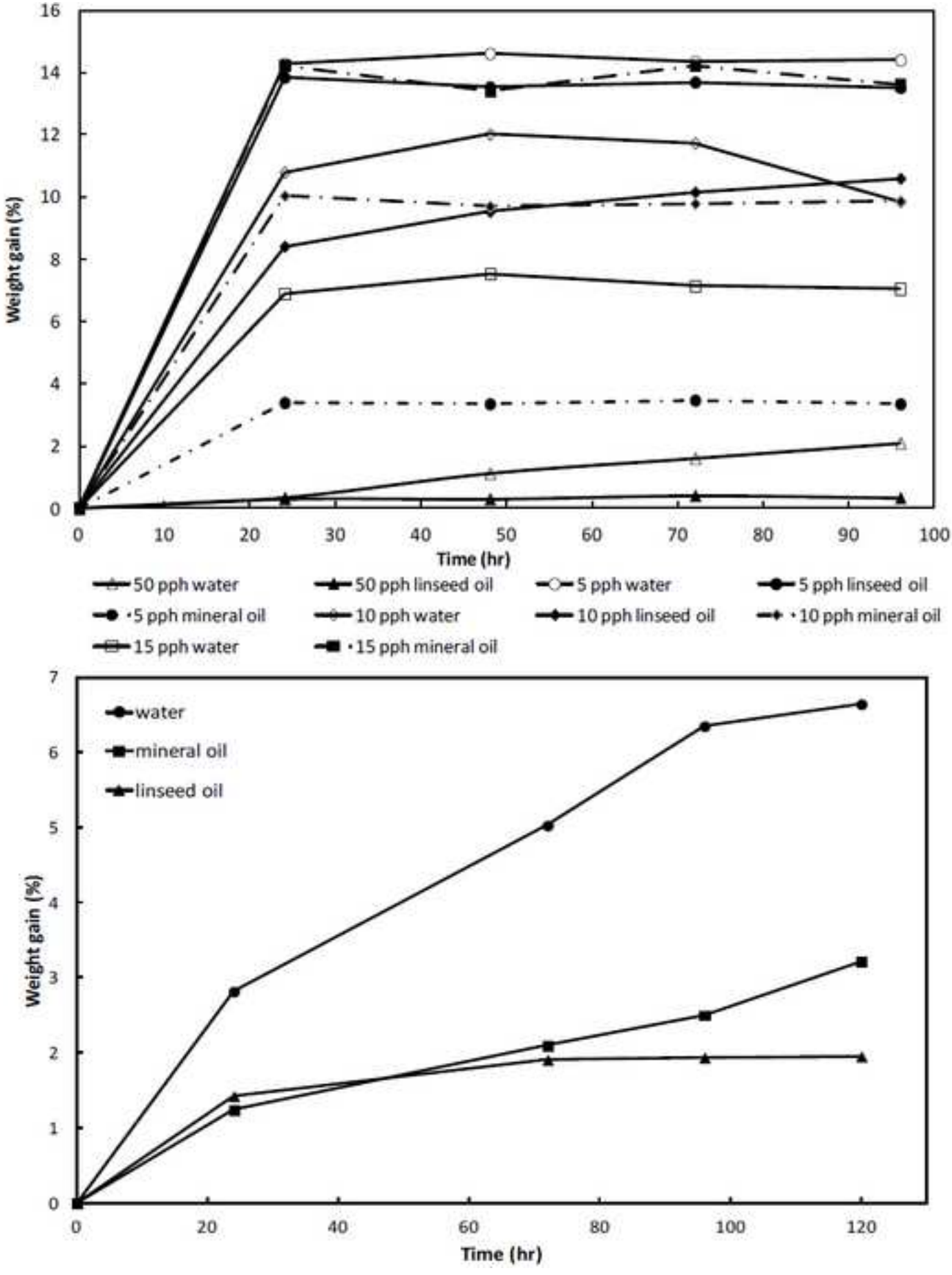

Figure 5 (SBR loss factor curves)
Click here to download high resolution image

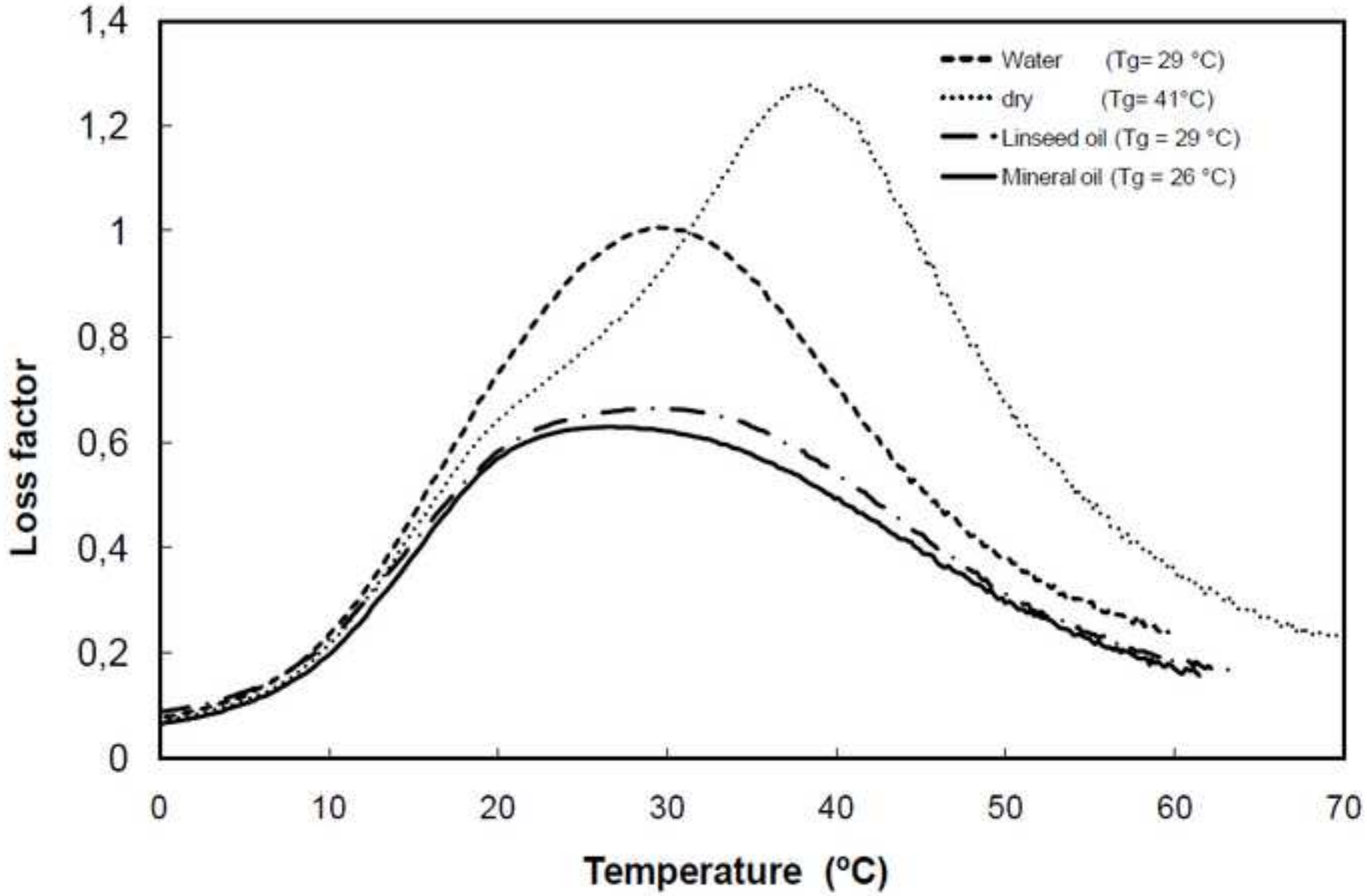

Figure 6 (SBR storage modulus curves)
Click here to download high resolution image

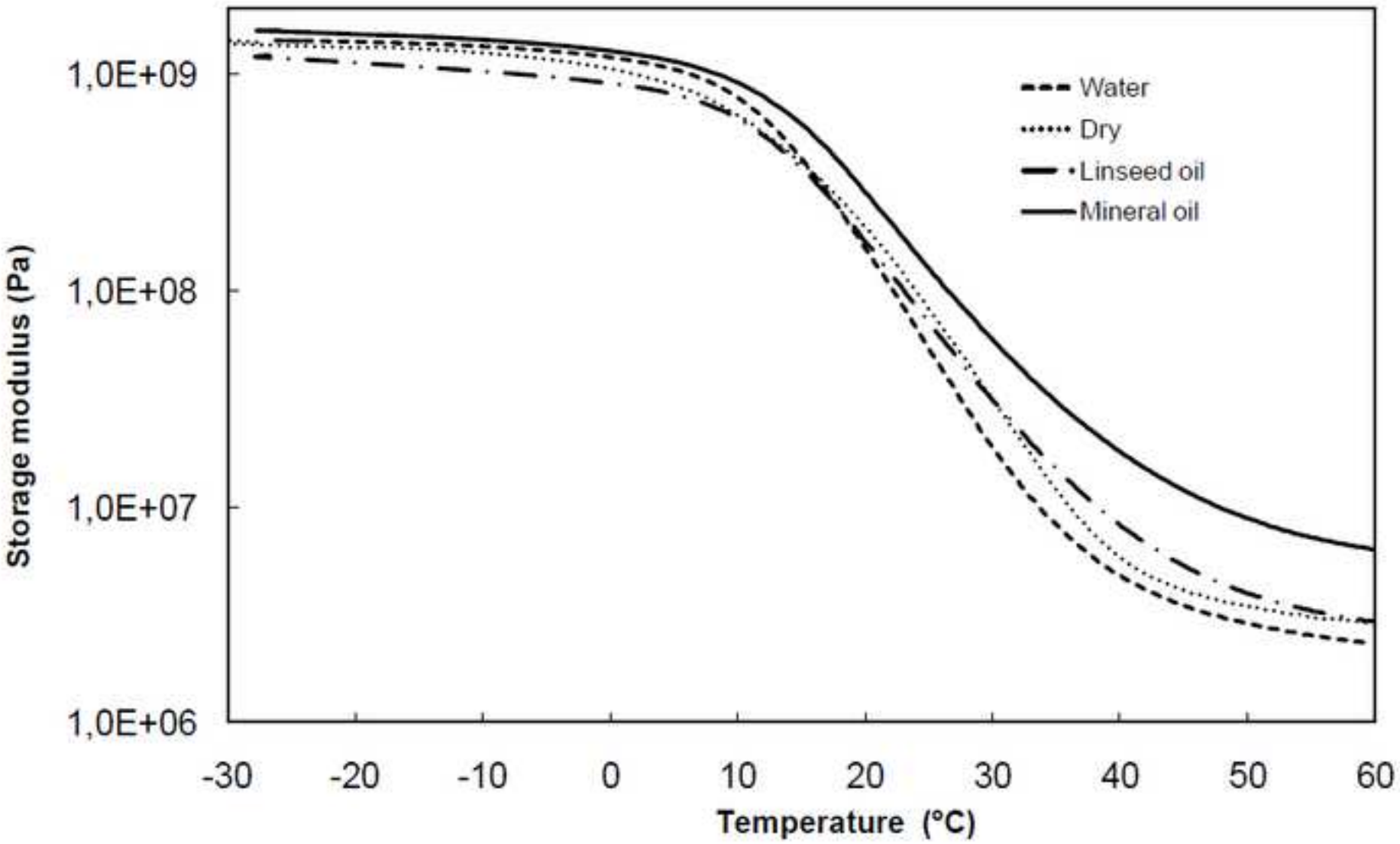

Figure 7 (effect of latex content on storage modulus in dry coa)
Click here to download high resolution image

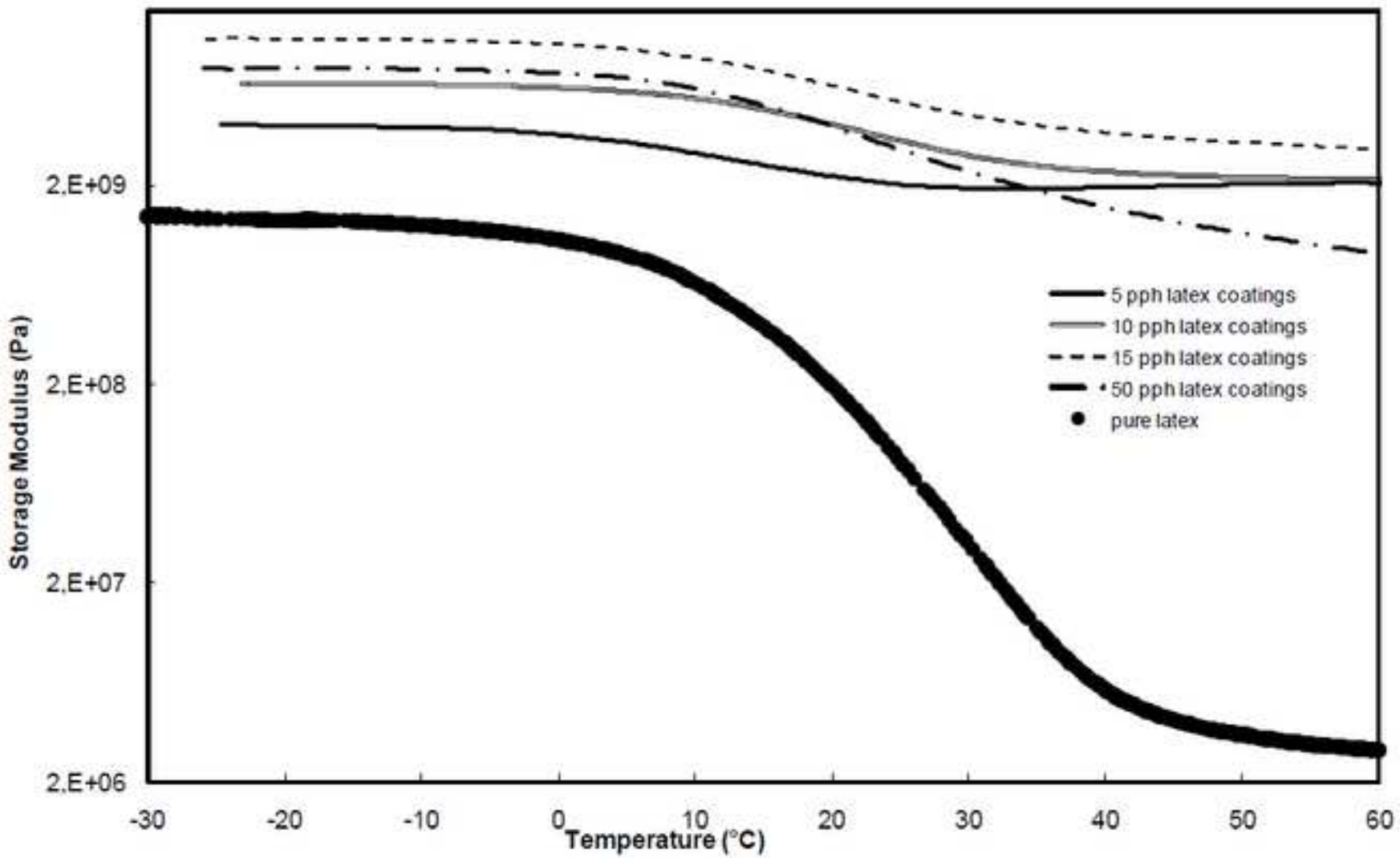

Figure 8 (storage modulus curves of 5 pph coatings dry and wet)
Click here to download high resolution image

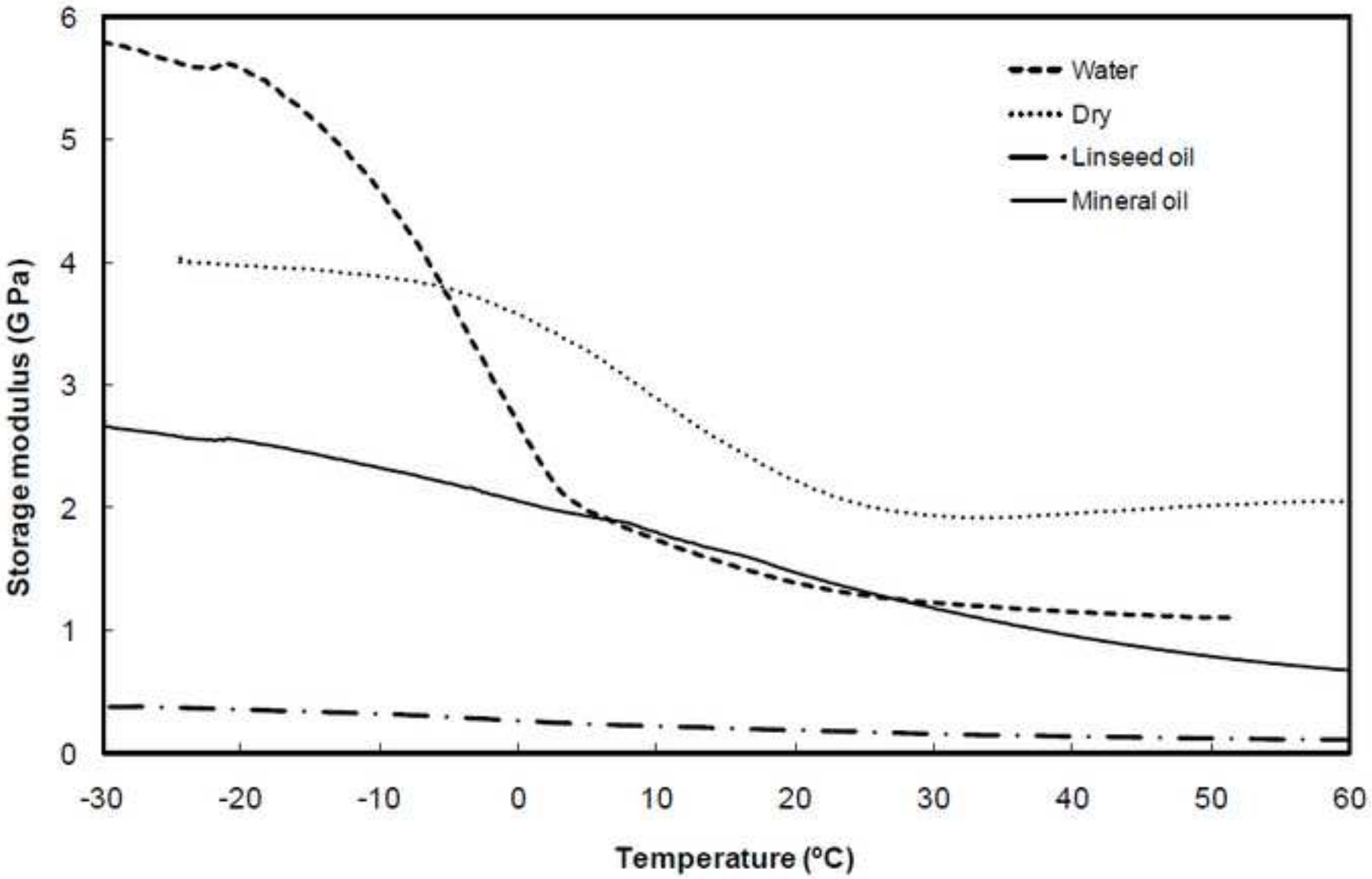

Figure 9 (loss factor curves of 5 pph coatings in dry and wet)
Click here to download high resolution image

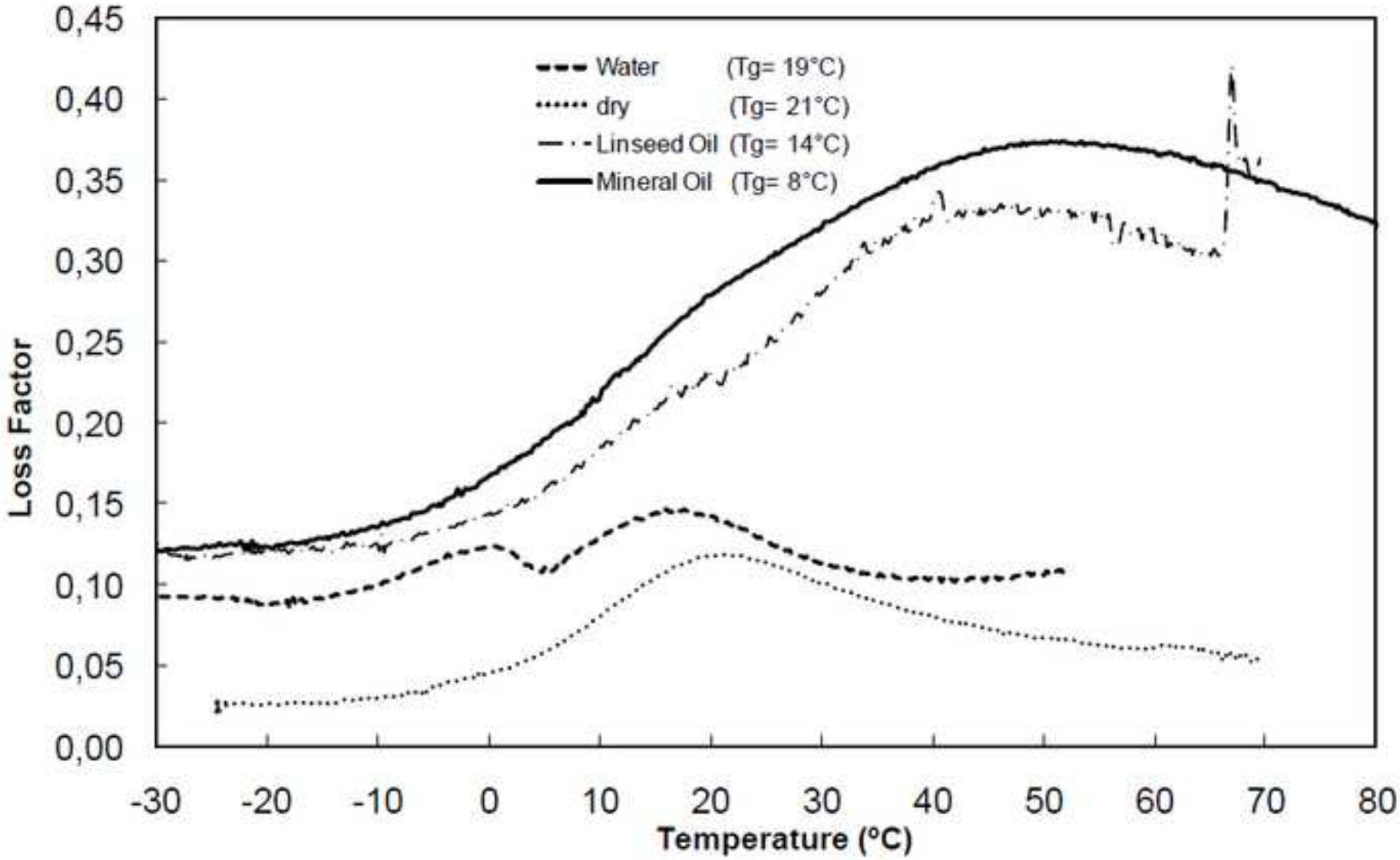

Figure 10 (curves of 10 pph storage modulus)
Click here to download high resolution image

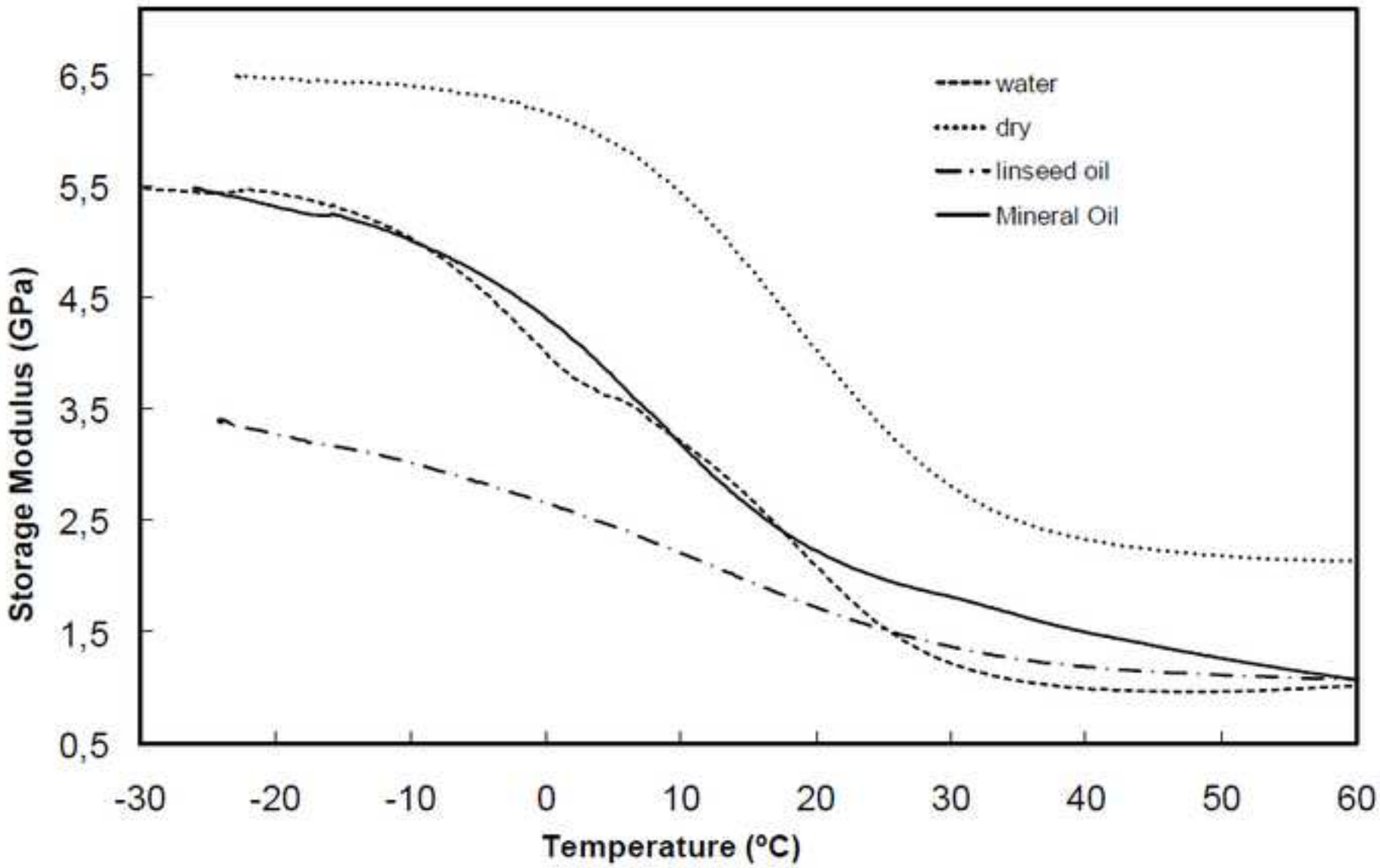

Figure 11 (curves of 10 pph loss factor)
Click here to download high resolution image

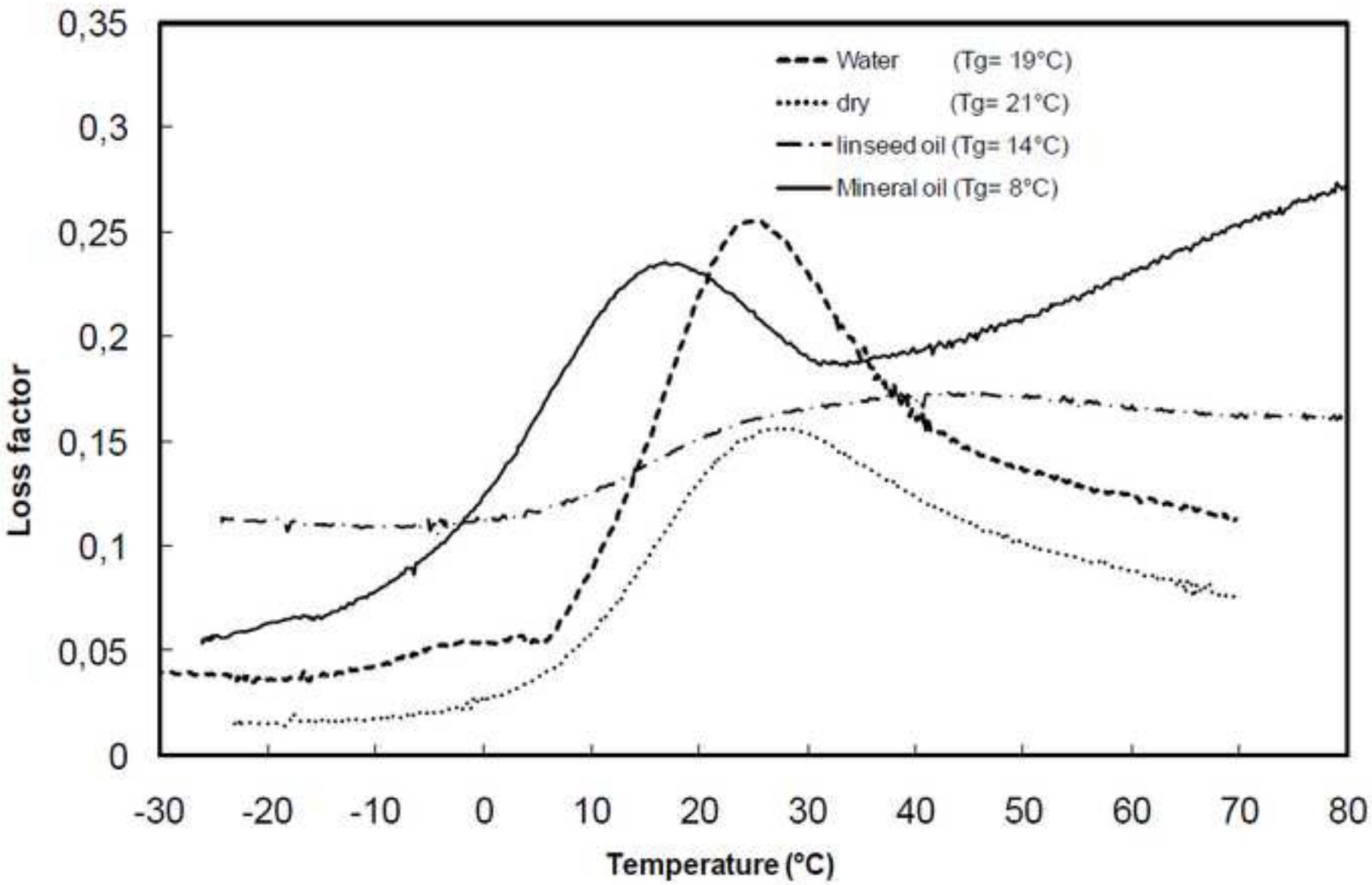

Figure 12 (curves of 15 pph storage modulus)
Click here to download high resolution image

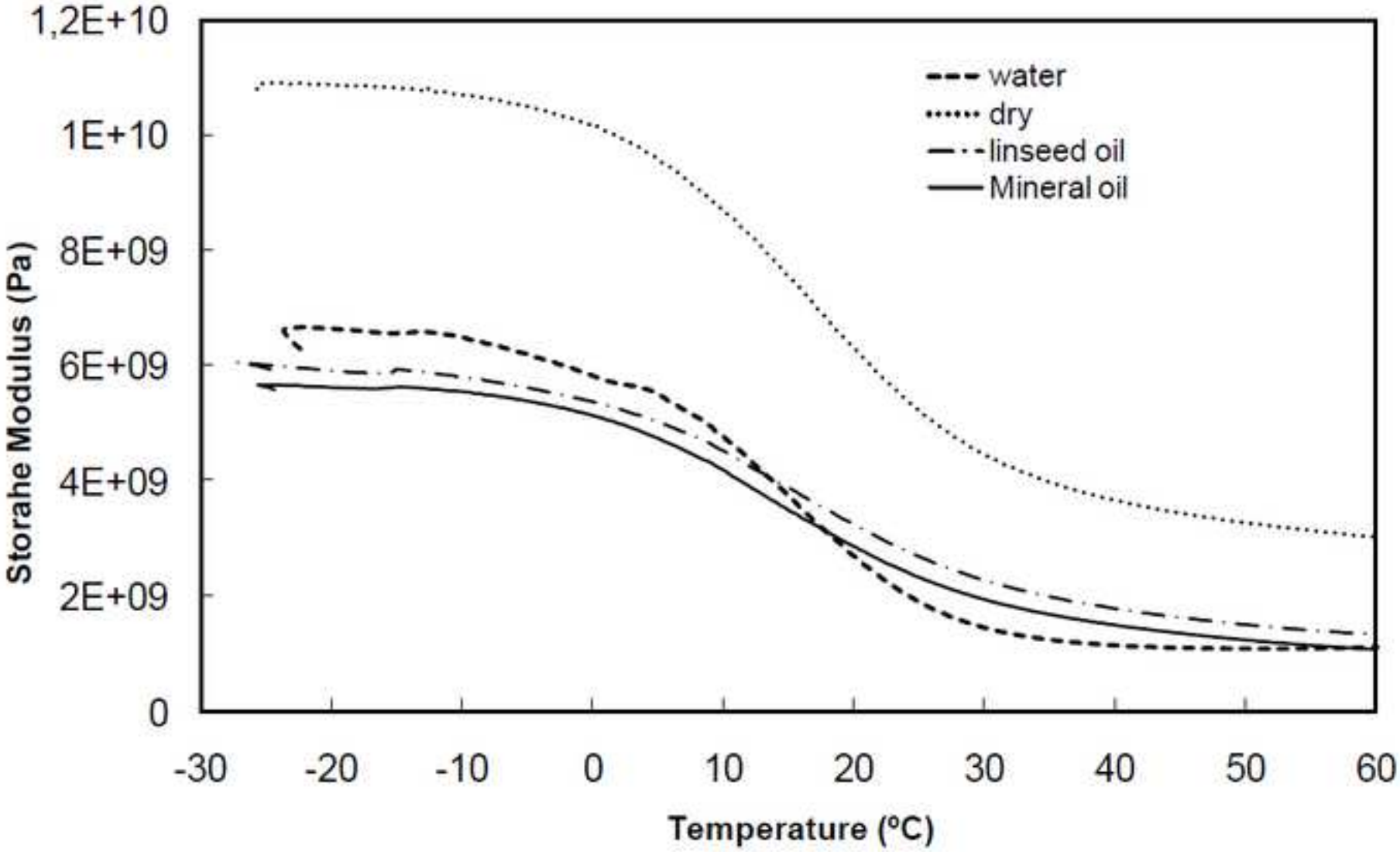

Figure 13 (curves of 15 pph loss factor)
Click here to download high resolution image

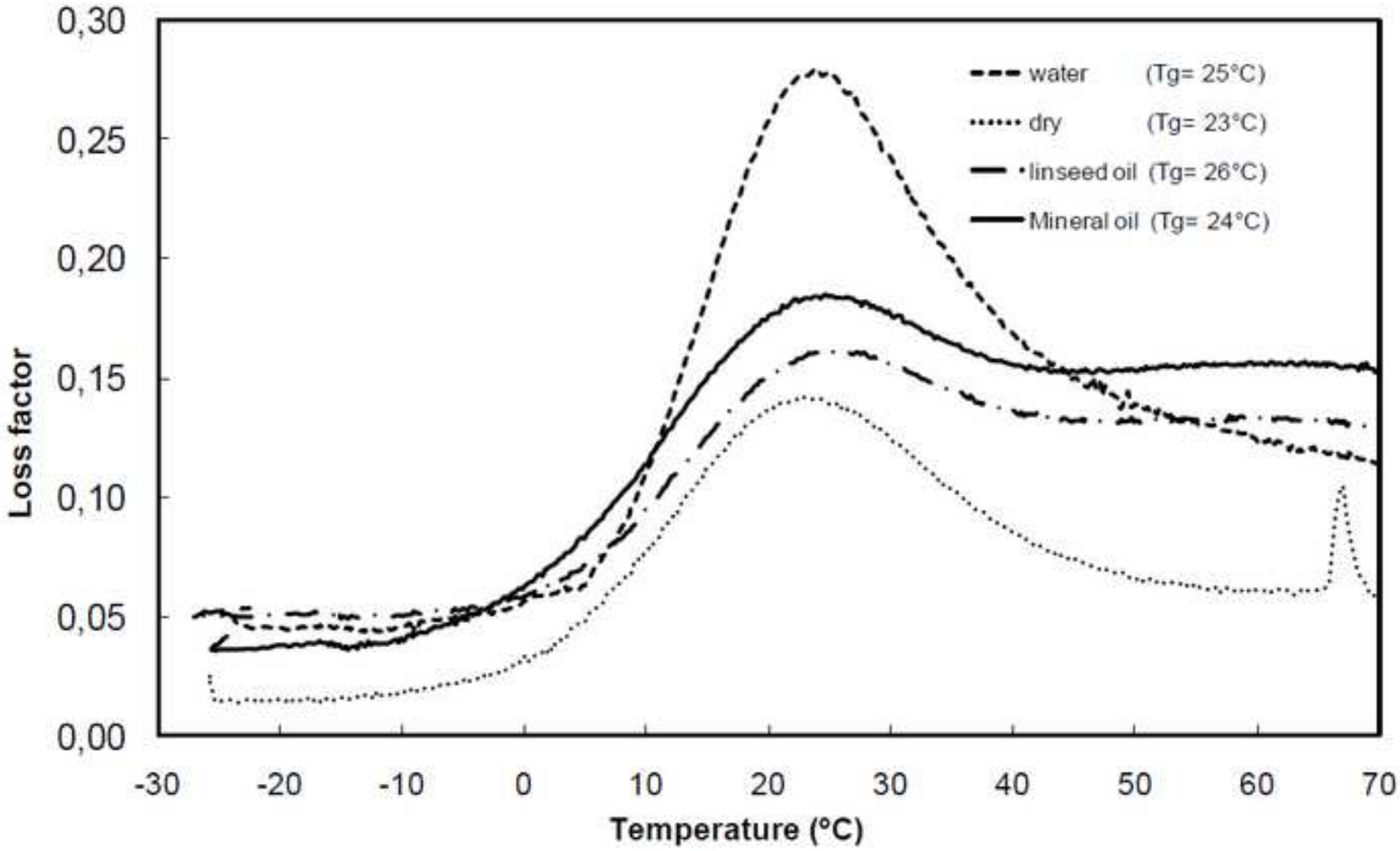

Figure 14 (curves of 50 pph storage modulus)
Click here to download high resolution image

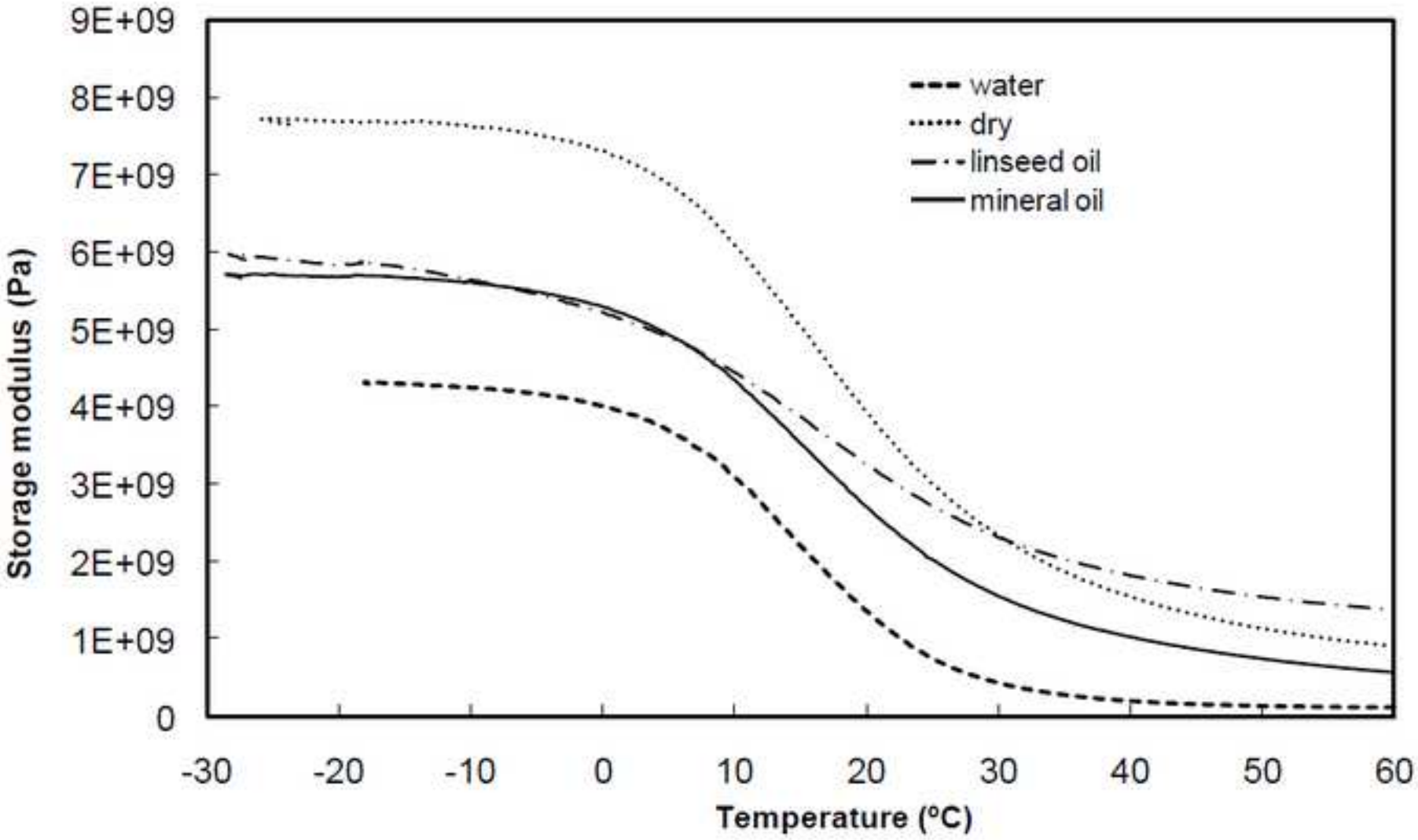

Figure 15 (curves of 50 pph loss factor)
Click here to download high resolution image

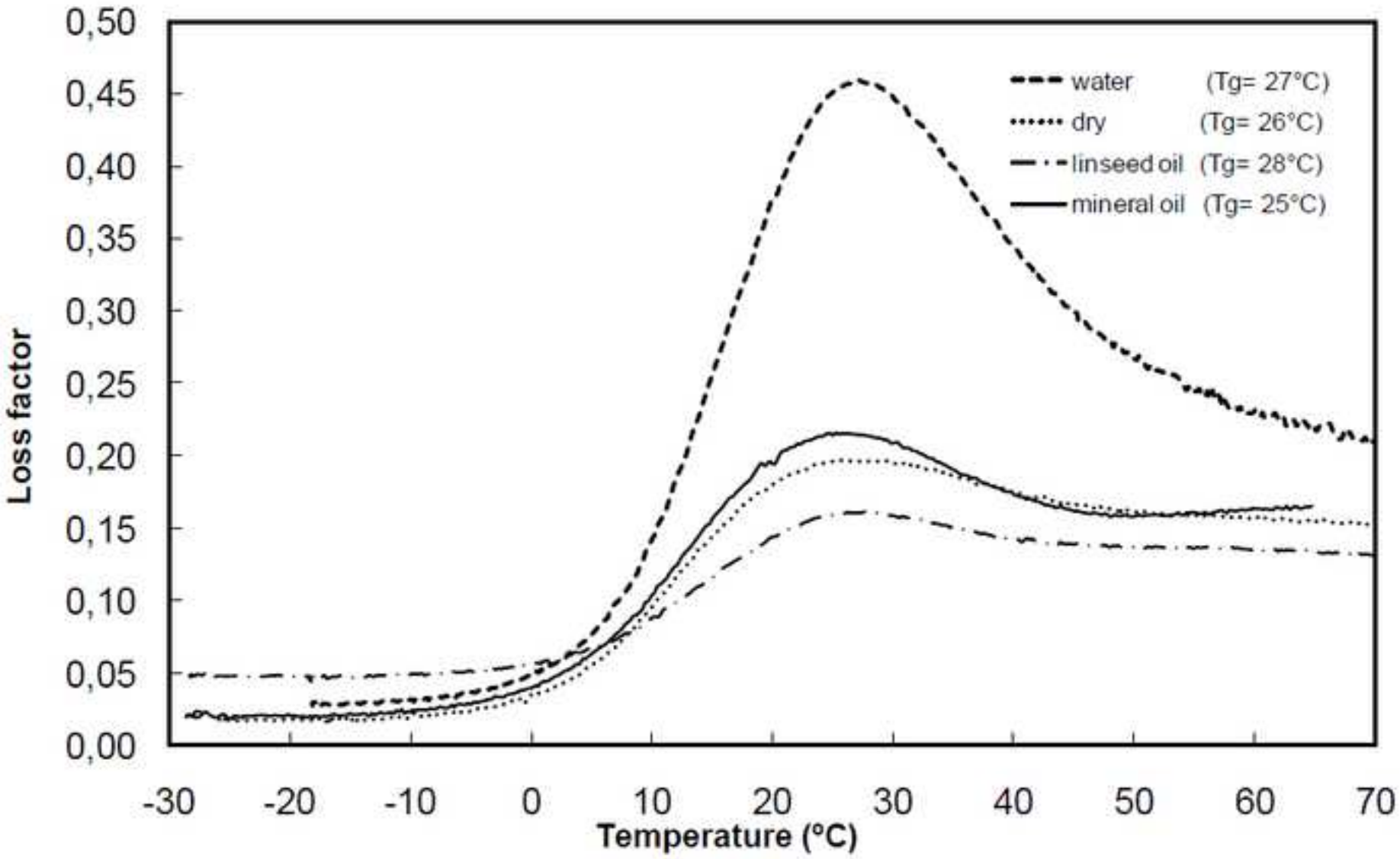

Figure 16 (solvent physicsl properties effects on storage modulu
Click here to download high resolution image

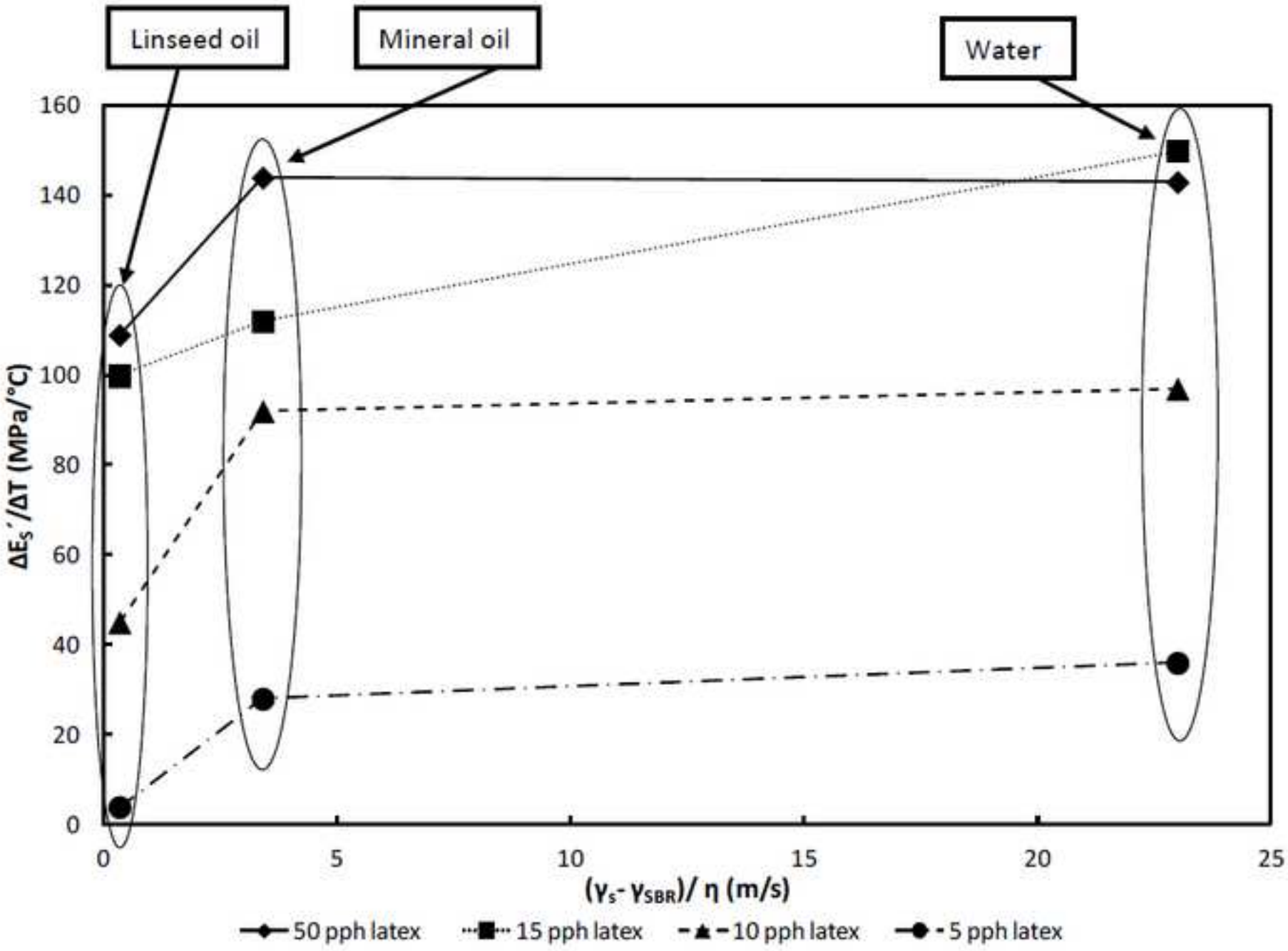

Figure 01. Example of BSEM image showing the microstructure of cross-section of 5 pph latex bulk coating, the pores, the calcium carbonate pigments and the latex are shown with red, blue and green arrows respectively.

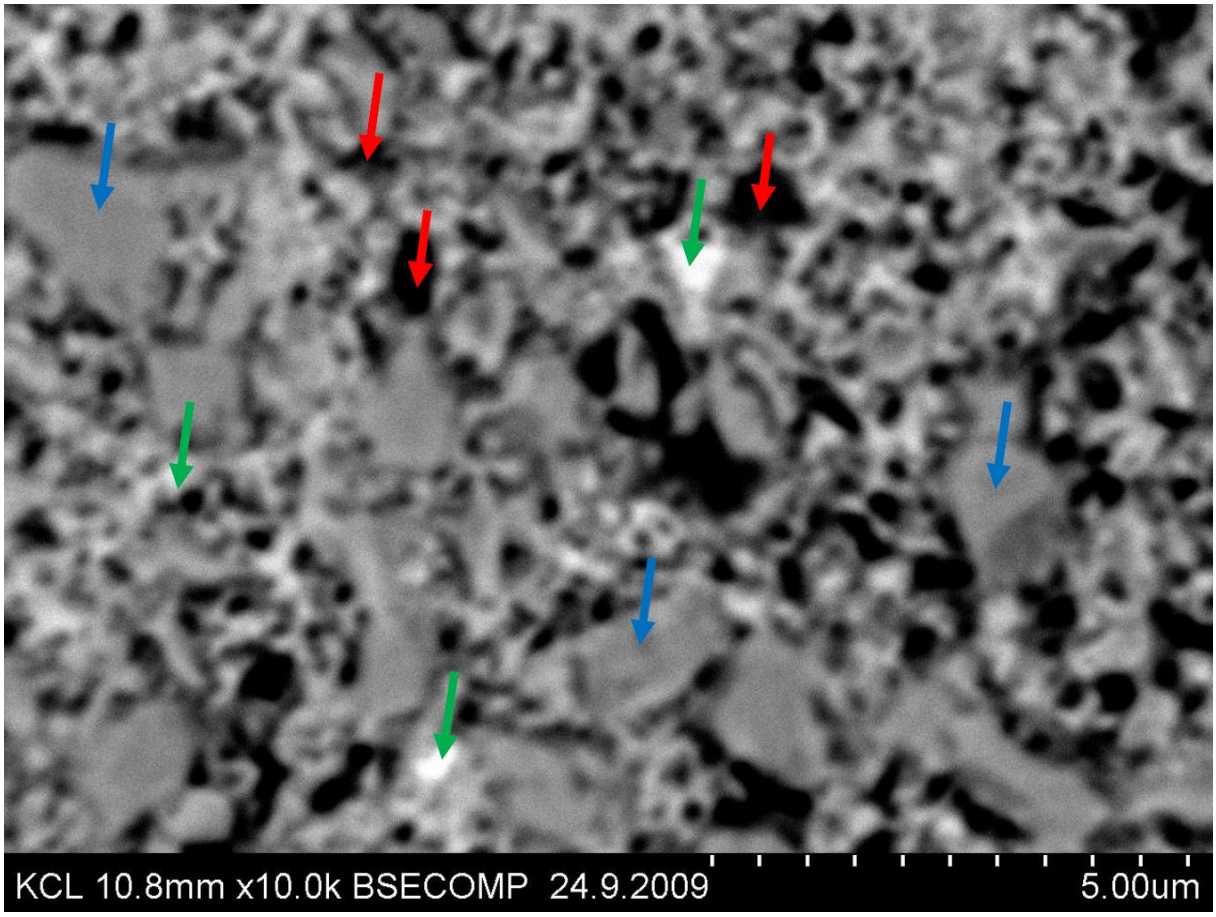

Figure.2: Example BSEM image showing the microstructure of cross section of 10 pph latex bulk coatings.

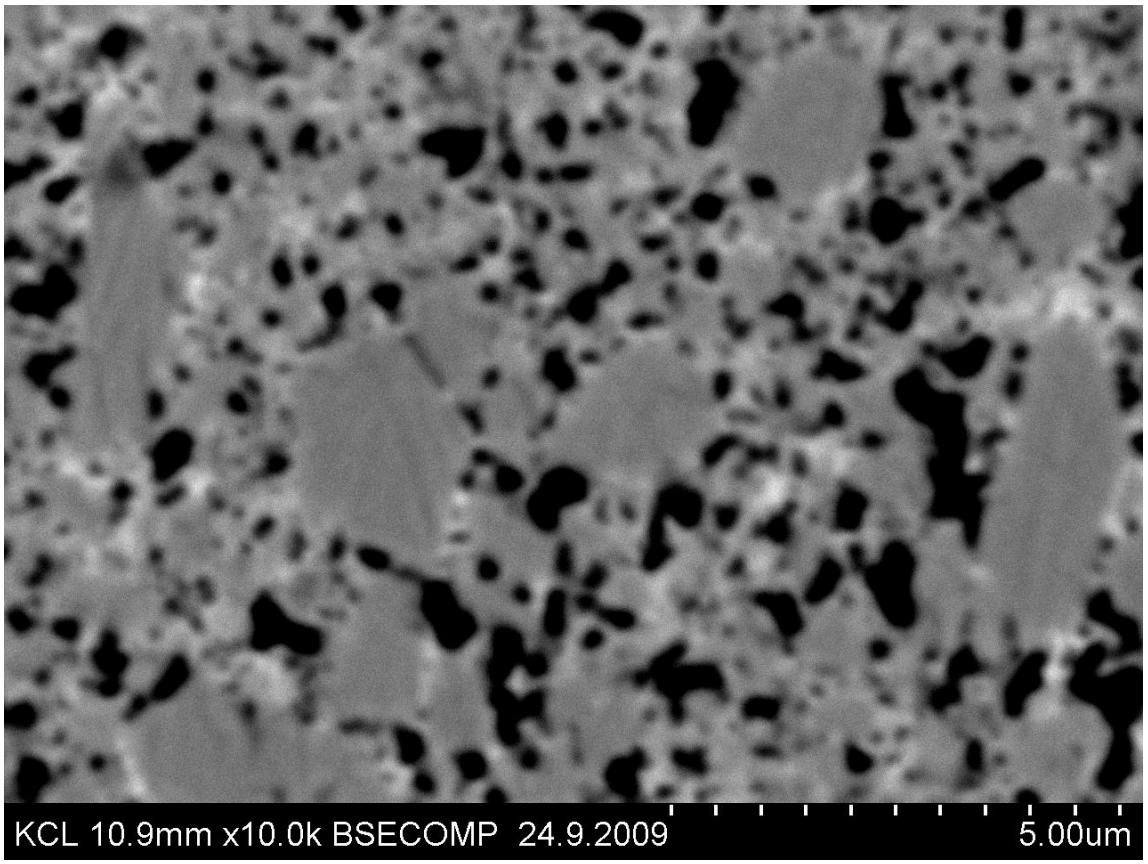

Figure(3)

Figure. 3: The pores distribution from Image J analysis software, upper image shows the 5 pph latex coatings where the lower shows the 10 pph coatings (magnification X10 000).

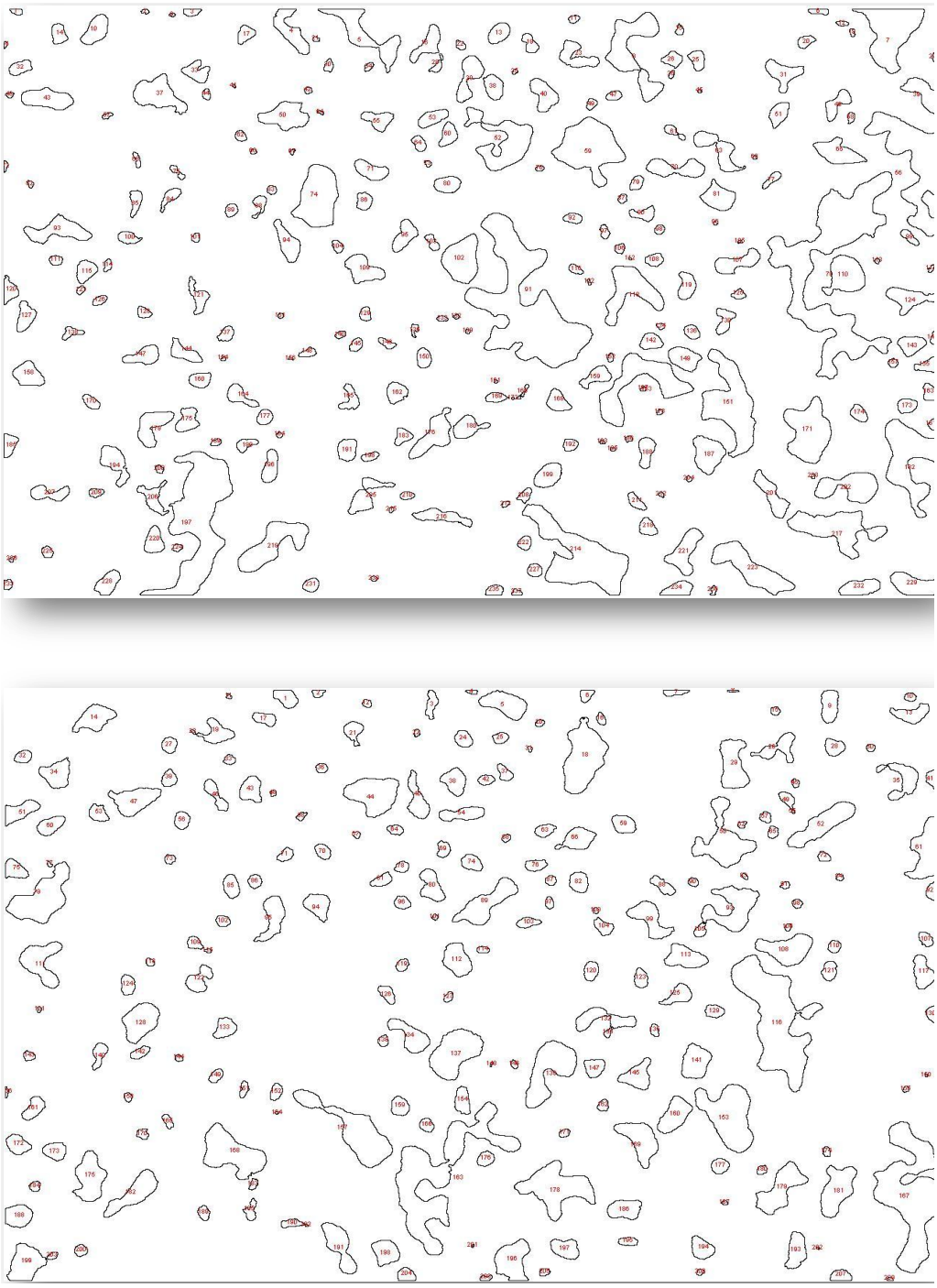

Figure(4)

Figure.4: Solvents absorption curves for composites (top) and pure latex samples (below).

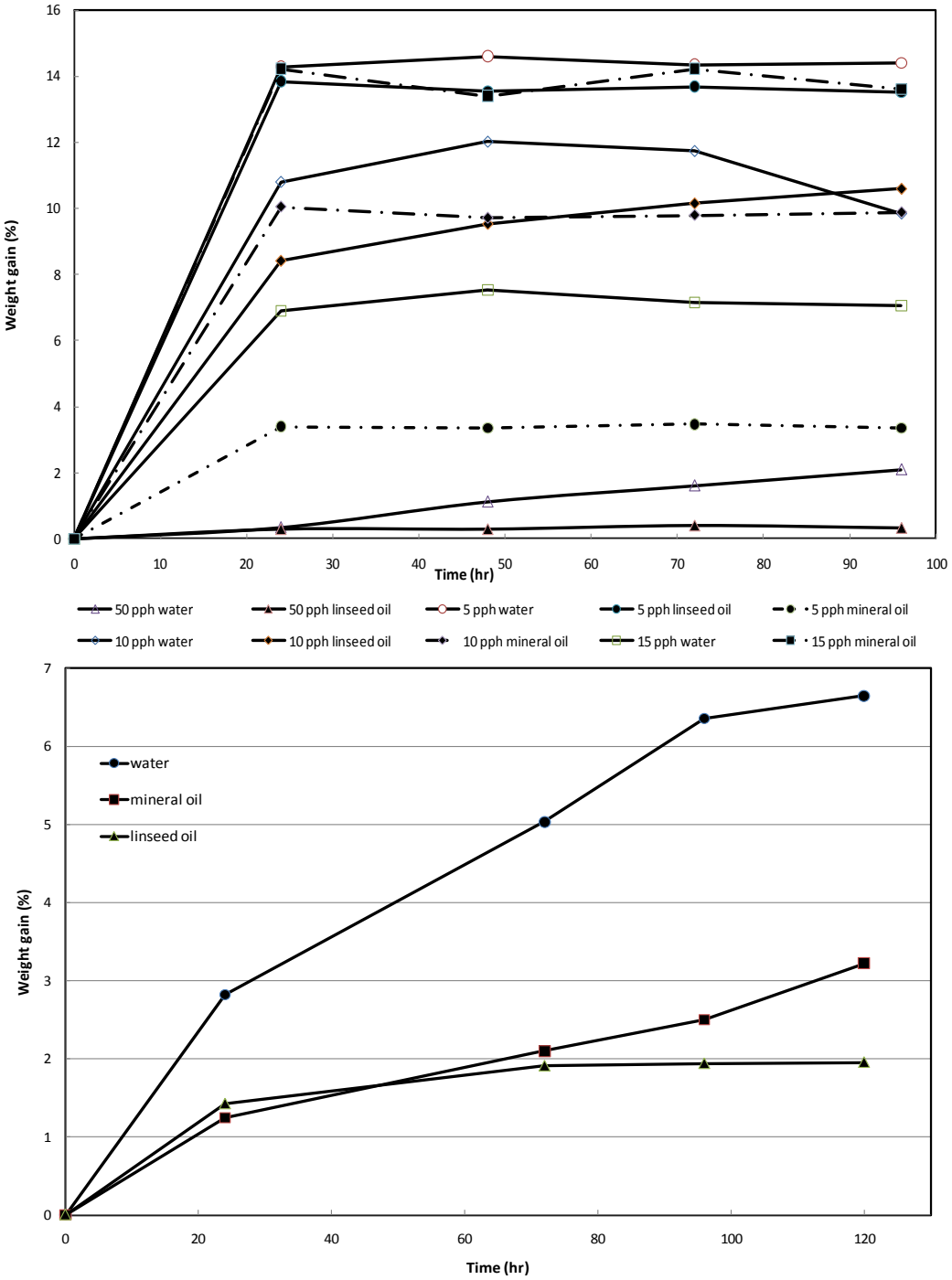

Figure(5)

Figure.5: Loss factor curves for pure SBR latex immersed in different solvents

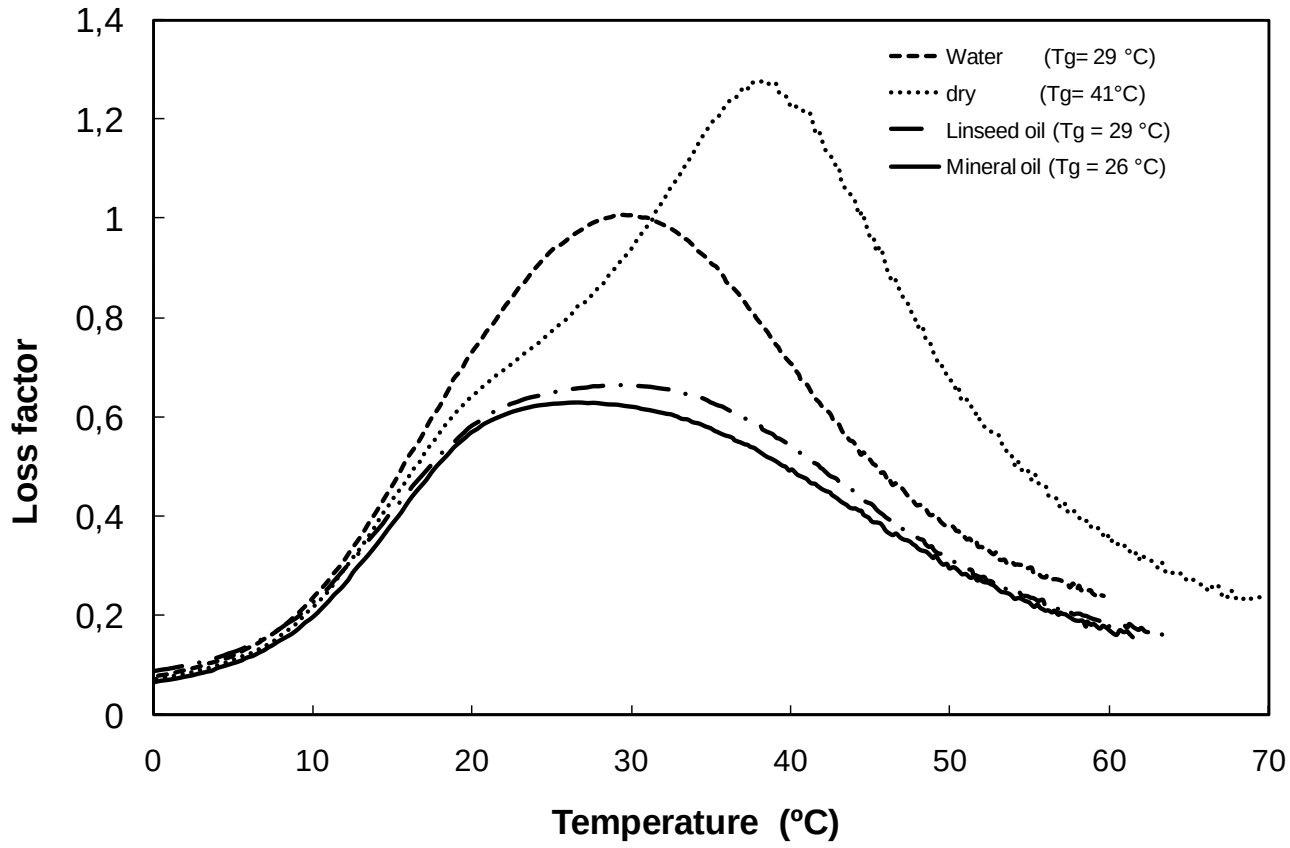

Figure(6)

Figure.6: Storage modulus curves for pure SBR latex immersed in different solvents.

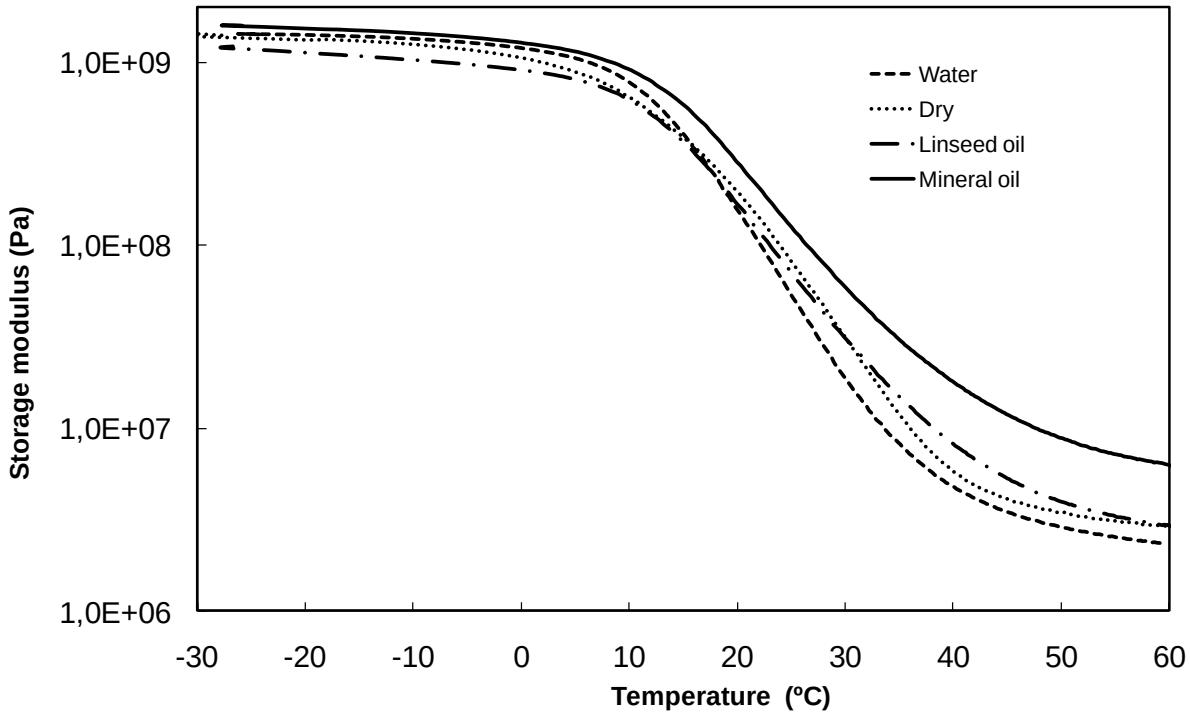

Figure(7)

Figure 7: Effect of latex volume fraction on storage modulus of dry coatings.

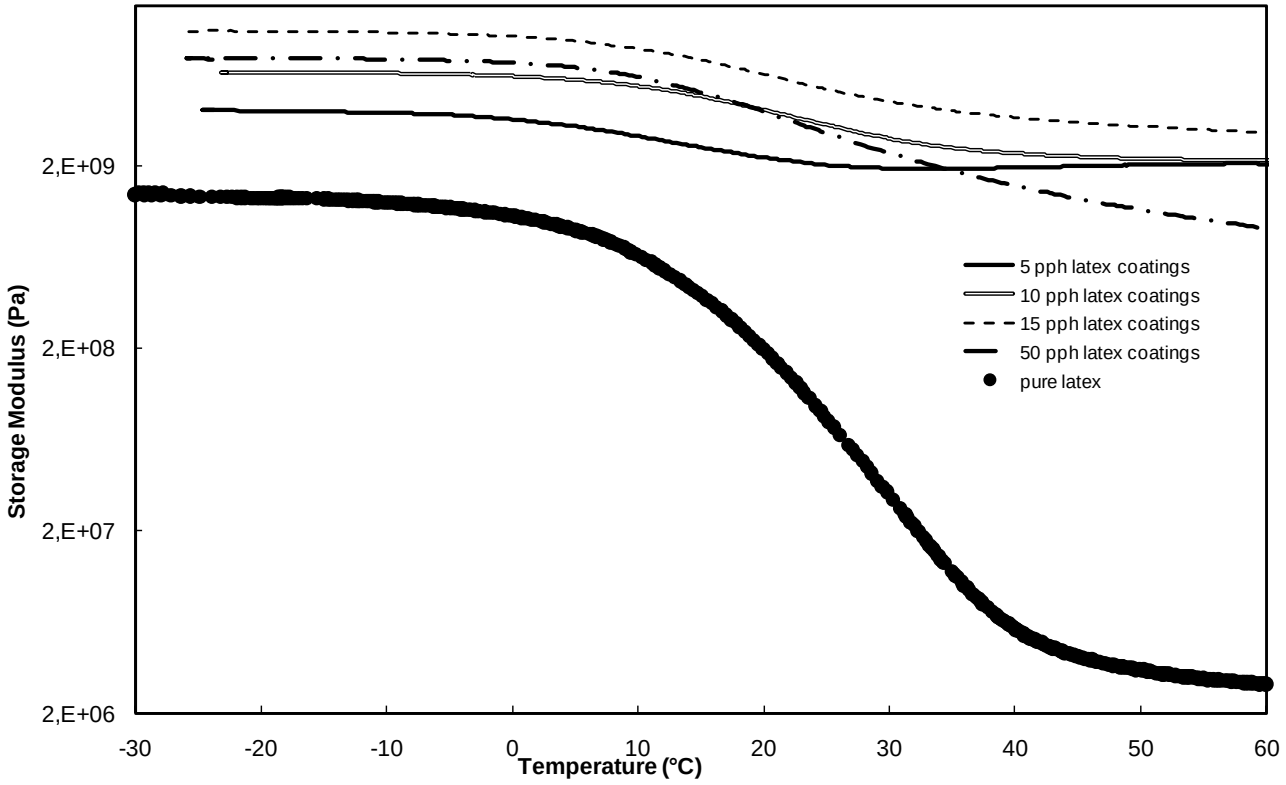

Figure(8)

Figure. 8. Storage modulus of 5 pph latex coatings as dry and as immersed in different solvents.

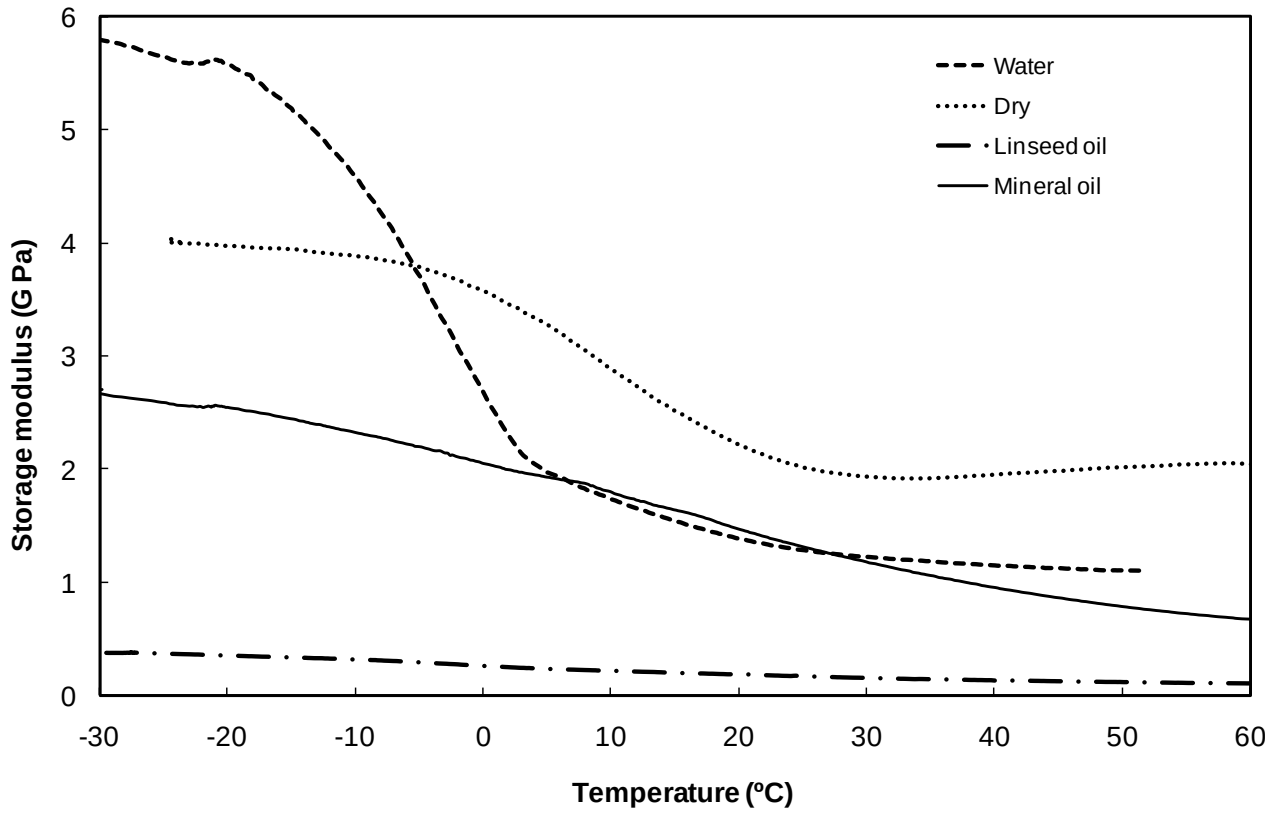

Figure(9)

Figure 9. Effect of water, mineral and linseed oils on the damping properties of 5 pph latex coatings.

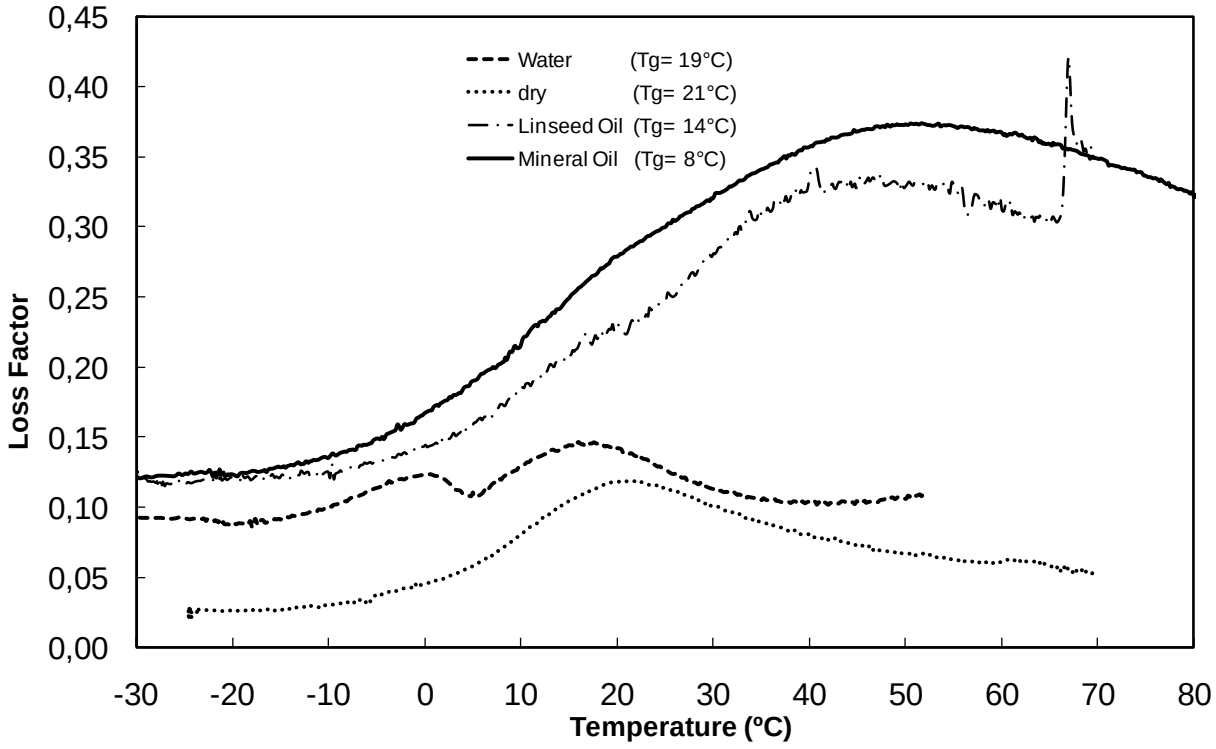

Figure(10)

Figure 10. Effect of different liquids on 10 pph latex coatings storage modulus.

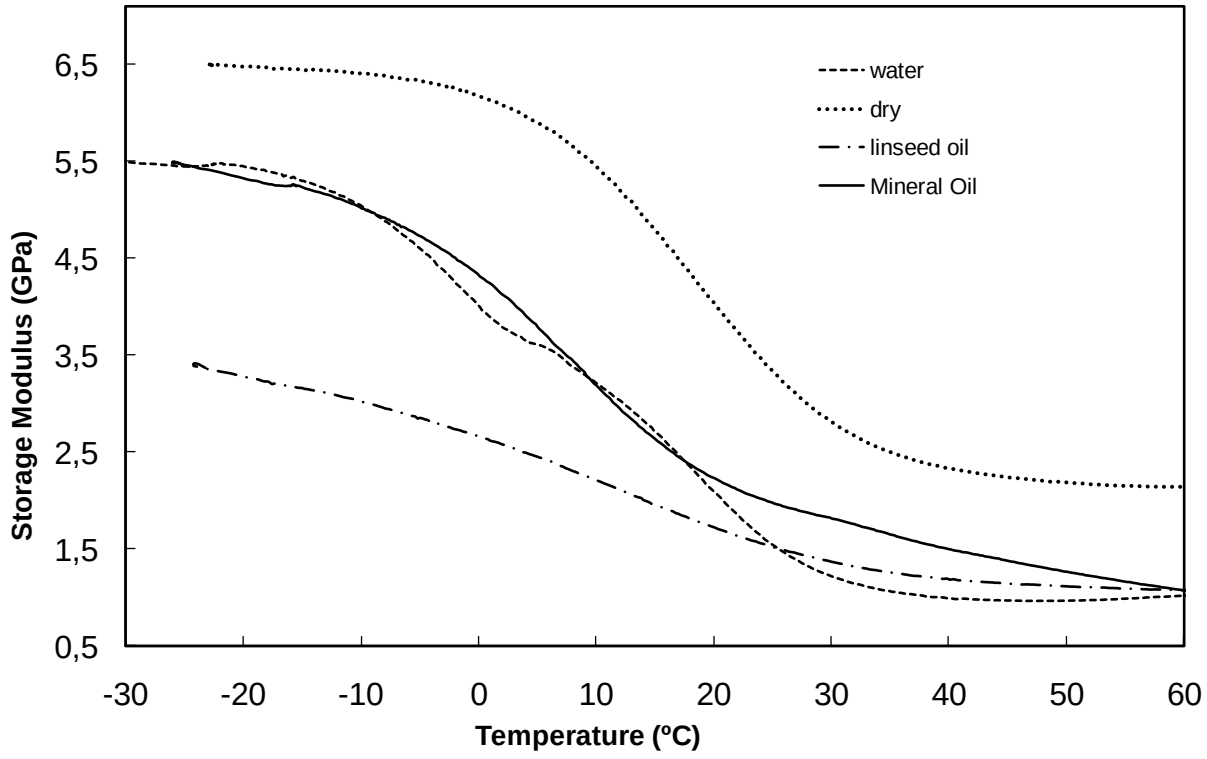

Figure(11)

Figure. 11. Effect of different solvents on the damping of 10 pph latex coatings.

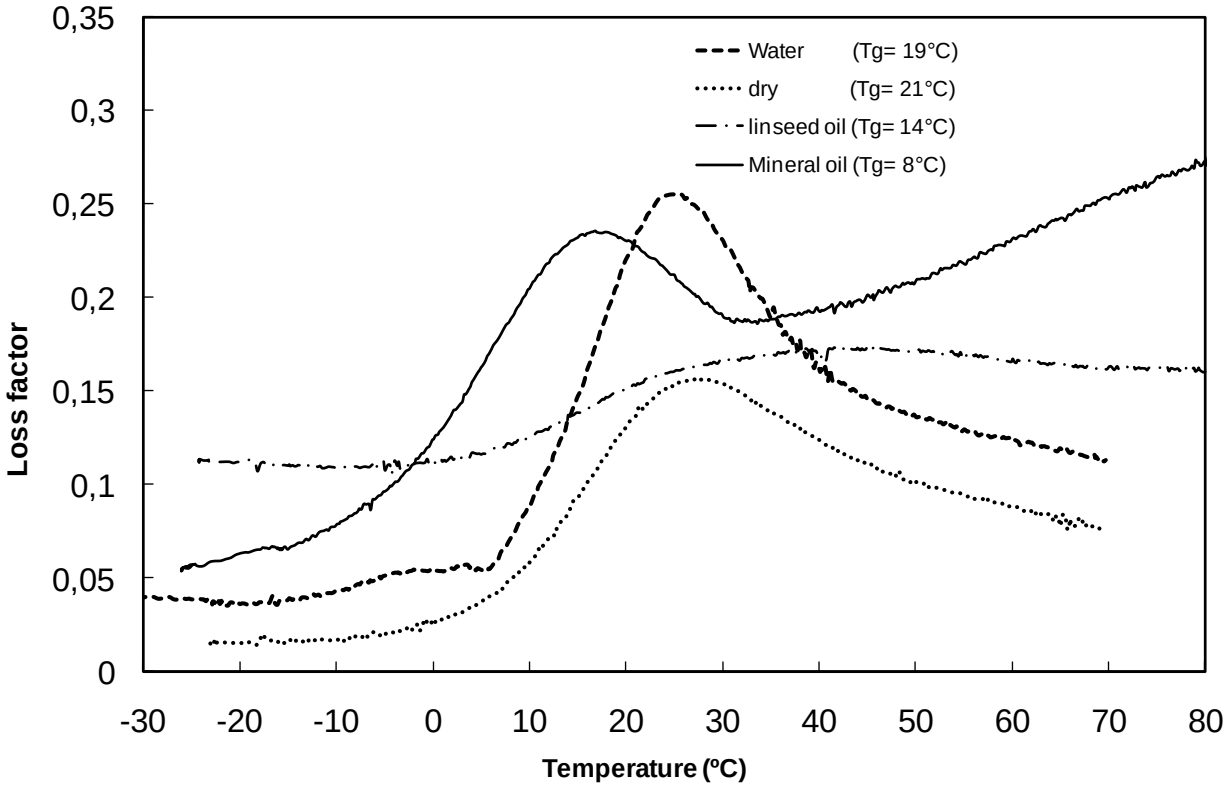

Figure(12)

Figure 12. Effect of different solvents on storage modulus of 15 pph latex coatings

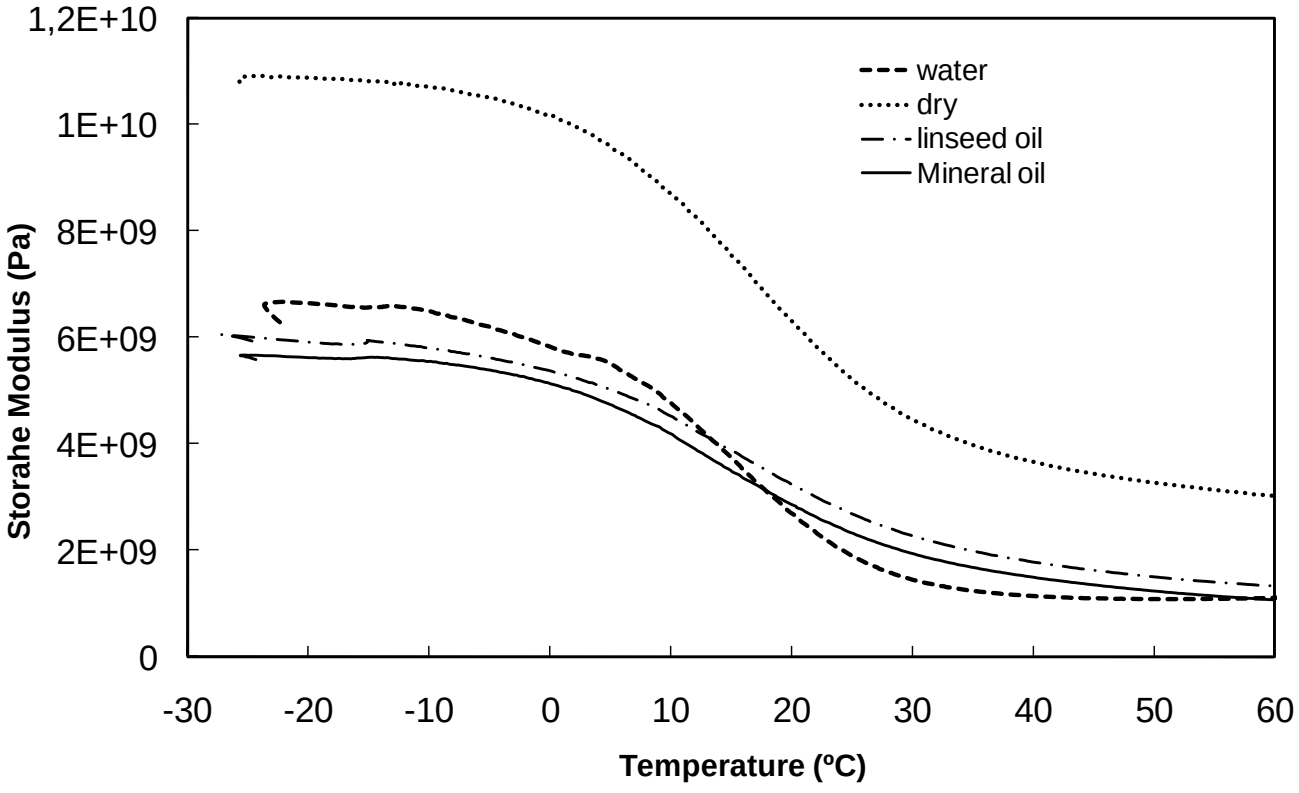

Figure(13)

Figure 13. Effect of different solvents on the damping of 15 pph latex coatings.

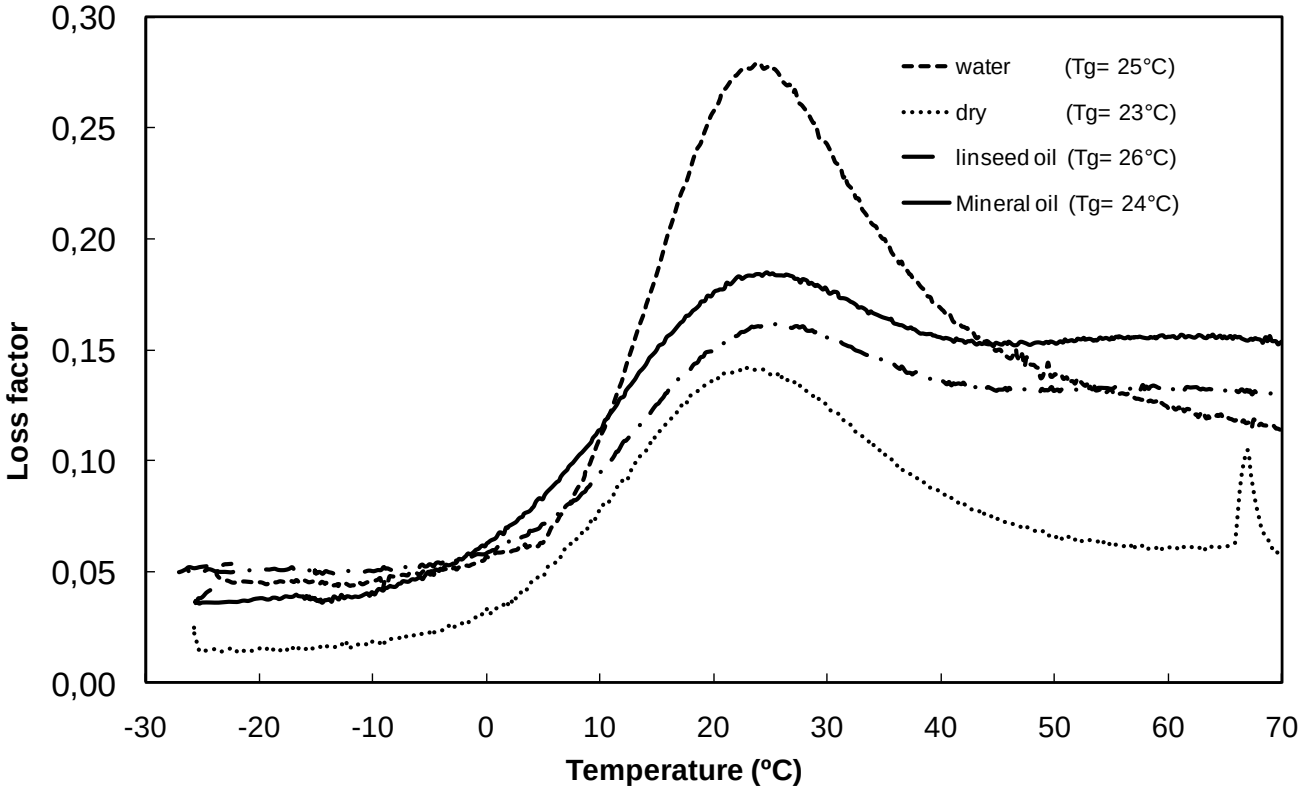

Figure(14)

Figure 14. The effect of water, linseed oil and mineral oil on the storage modulus for 50 pph latex coatings.

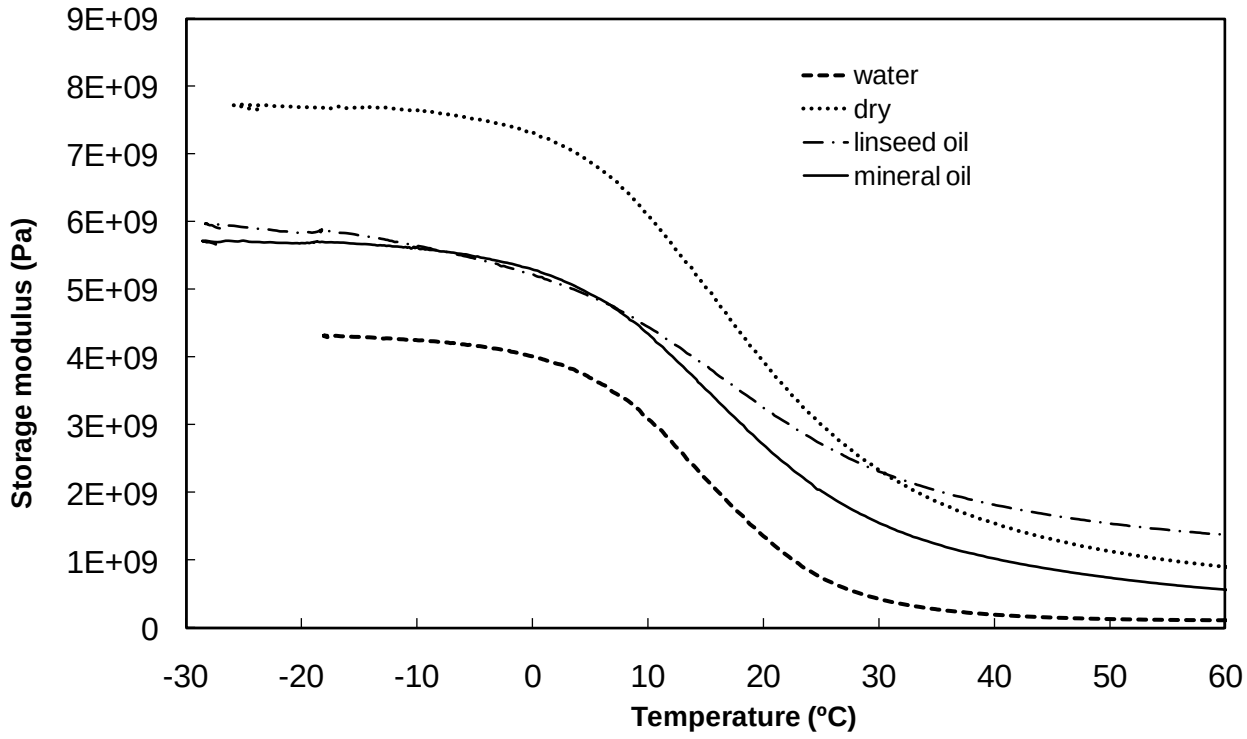

Figure(15)

Figure 15: The effect of solvents on the damping properties of 50 pph latex coatings.

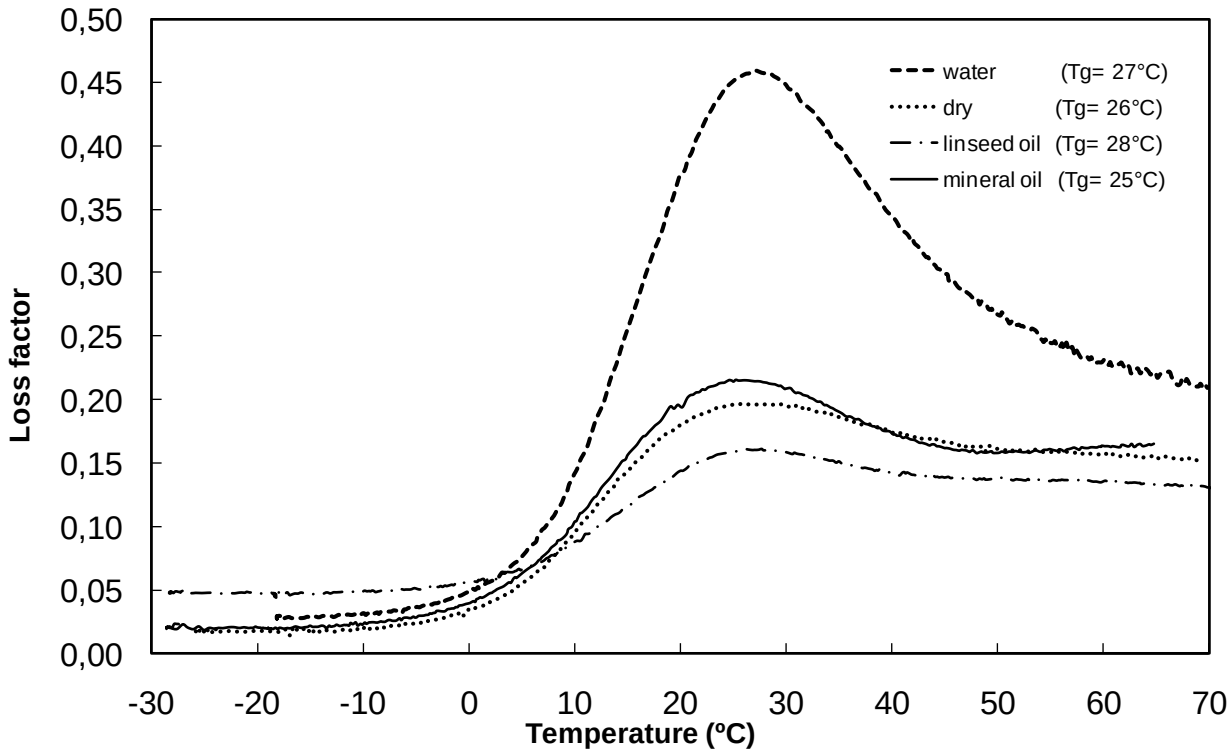

Figure(16)

Figure.16. Effect of solvent physical properties on storage modulus drop for different coatings.

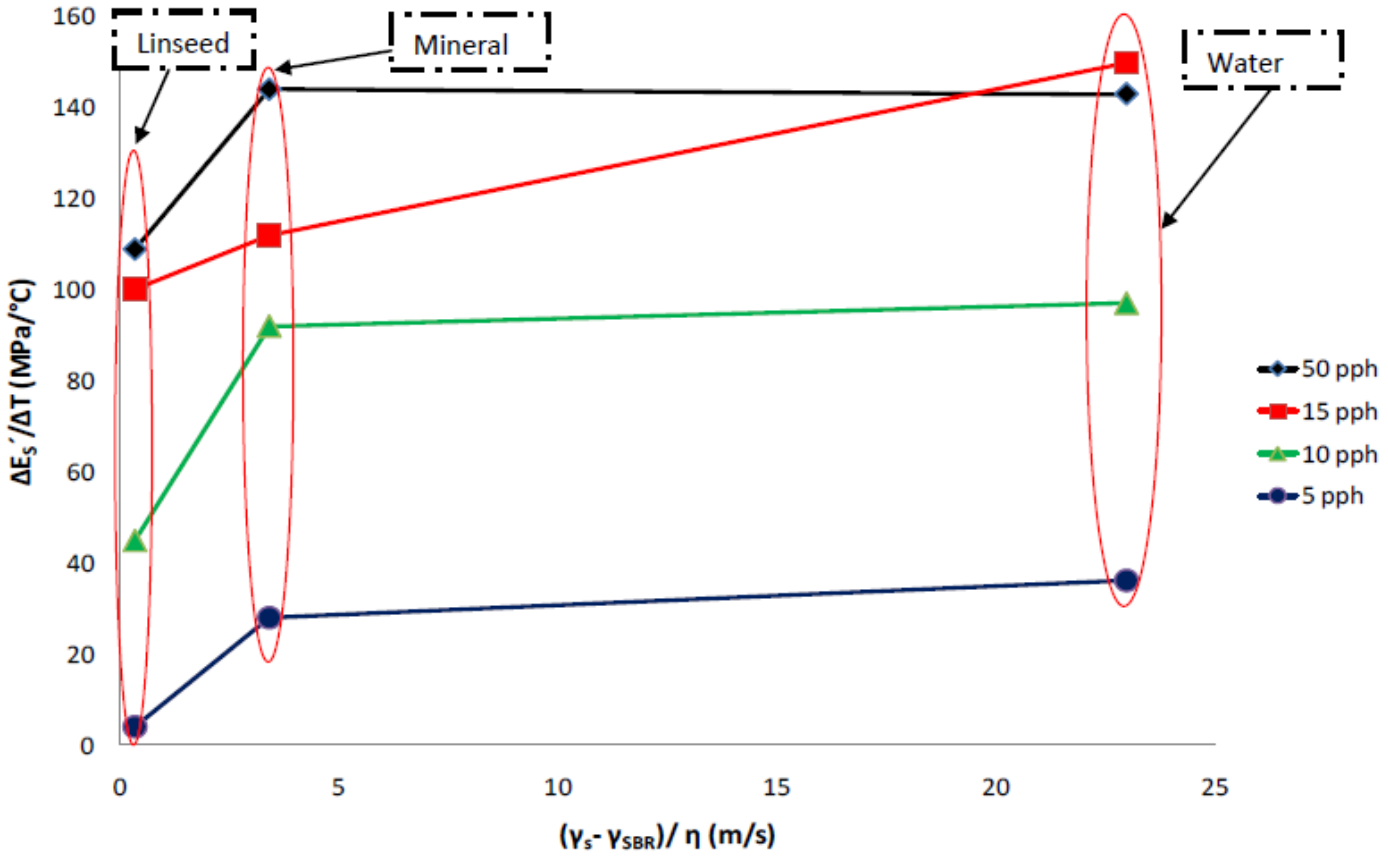

Table 1. Some physical properties of latex and different solvents used in this study

	Viscosity at RT η (mPas)	Surface tension γ (mN/m)	$(\gamma_s - \gamma_{SBR})/ \eta$ (m/s)	Density (g/cm^3)
Water	**1**	**72**	**15**	**1**
Linseed oil	**45.1**	**34**	**0,5**	**0.928**
Mineral oil	**6**	**28.5**	**4,8**	**0.827**
Styrene butadiene acrylic acid latex	**-**	**57±8**	**-**	**1.03**

Table2

Table 2. Image J analysis of 5 pph latex and 10 pph BSEM images

	5 pph coatings (bulk)	10 pph coatings (bulk)
Pore area fraction (%)	21.4	13.72
Average pore size (μm^2)	0.119	0.074
Number of pores	204	193
Circularity	0.666	0.716
Feret's Diameter (µm)	0.441	0.361

Table(1)

Table 1. Some physical properties of latex and different solvents used in this study

	Viscosity at RT η (mPas)	Surface tension γ (mN/m)	$(\gamma_s - \gamma_{SBR})/ \eta$ (m/s)	Density (g/cm^3)
Water	**1**	**72**	**15**	**1**
Linseed oil	**45.1**	**34**	**0,5**	**0.928**
Mineral oil	**6**	**28.5**	**4,8**	**0.827**
Styrene butadiene acrylic acid latex	**-**	**57±8**	**-**	**1.03**

Table(2)

Table 2. Image J analysis of 5 pph latex and 10 pph BSEM images

	5 pph coatings (bulk)	10 pph coatings (bulk)
Pore area fraction (%)	**21.4**	**13.72**
Average pore size (μm^2)	**0.119**	**0.0746**
Number of pores	**204**	**193**
Circularity	**0.6665**	**0.7166**
***Feret's Diameter* (µm)**	**0.44175**	**0.361**